


For Reference

NOT TO BE TAKEN FROM THIS ROOM

Ex LIBRIS
UNIVERSITATIS
ALBERTAENSIS





Digitized by the Internet Archive
in 2023 with funding from
University of Alberta Library

<https://archive.org/details/Pajkowski1973>

THE UNIVERSITY OF ALBERTA

NEXT NEAREST NEIGHBOUR INTERACTIONS IN LATTICE STATISTICS

by



HENRY ROBERT PAJKOWSKI

A THESIS

SUBMITTED TO THE FACULTY OF GRADUATE STUDY AND RESEARCH
IN PARTIAL FULFILMENT OF THE REQUIREMENTS FOR THE DEGREE
OF MASTER OF SCIENCE

DEPARTMENT OF PHYSICS

EDMONTON, ALBERTA

FALL, 1973

ABSTRACT

Next nearest neighbour interactions are introduced for two different lattice models. The canonical partition function of the one-dimensional spin $\frac{1}{2}$ Ising model in zero field with nearest (J_1) and next nearest (J_2) neighbour interactions is evaluated. The locus of zeros of this partition function is then found for different ratios of J_2 to J_1 . We also consider a one-dimensional Heisenberg model in zero field with nearest and next nearest interactions, J_1 and J_2 respectively, as before. Repeating the work of Niemeijer, a temperature-dependent Hartree-Fock approximation is used to obtain a trial Helmholtz free energy per site, which is an upper bound for the true free energy per site. The resulting equations can be solved at zero temperature for an approximate ground state wavefunction; the corresponding energy per site is an upper bound for the exact ground state energy per site. Several cases are looked at, for different relative values of J_1 and J_2 . For $J_1 > 0$ part of the upper bound for the ground state energy per site which was overlooked by Niemeijer is obtained. Also, asymptotes to the energy upper bound for J_1 greater than and less than zero are found.

ACKNOWLEDGMENTS

Many thanks are due to my Supervisor, Dr. John Stephenson, for suggesting the project and for his invaluable assistance and encouragement throughout.

Financial assistance from the National Research Council of Canada, via a Postgraduate Bursary, and the Department of Physics, University of Alberta, through a Graduate Assistantship, are gratefully acknowledged.

Finally, I wish to express my appreciation to my then fiancée and now wife, Dianne, for her understanding and encouragement and for assistance in typing this Thesis.

TABLE OF CONTENTS

CHAPTER		PAGE
I	INTRODUCTION	1
II	ONE-DIMENSIONAL SPIN $\frac{1}{2}$ ISING MODEL	4
	1. Preliminaries	4
	2. Zeros of Partition Function	7
	3. Numerical Results	13
	4. Discussion of Numerical Results	23
	A. Properties of Solutions -- The General Case	23
	B. Exactly Soluble Cases	30
	C. Other Special Cases	33
III	ONE-DIMENSIONAL SPIN $\frac{1}{2}$ HEISENBERG MODEL ..	35
	1. Preliminaries	35
	2. Calculation of Single-Particle Energy, $\epsilon(k)$	38
	3. Solution for $T = 0$	49
	A. Ferromagnetic NN Interactions	53
	B. Antiferromagnetic NN Interactions.	71
IV	CONCLUSION	83

TABLE OF CONTENTS (Cont'd.)

	PAGE
BIBLIOGRAPHY	85
APPENDIX	87

LIST OF TABLES

TABLE	DESCRIPTION	PAGE
1	Solutions of (3 - 50) for various α , with corresponding E'_t	63
2	Solutions of (3 - 73) for various α , with corresponding E'_t	76

LIST OF FIGURES

FIGURE		PAGE
1, 2, 3, 4, 5 and 6	Locus of zeros of partition function (2 - 16) in complex fugacity plane for various λ	16
7	The interval I	51
8	$\epsilon(k)$, equations (3 - 40), as function of ϕ_k for $I = 0$, i.e. $x = y$, for different ranges of α with $J_1 < 0$	58
9	Elementary excitation spectrum, $\epsilon(k)$, as function of ϕ_k for different ranges of α with $J_1 < 0$	60
10	Upper bounds for exact ground state energy per site for infinite chain with $J_1 < 0$, as function of α	65

LIST OF FIGURES (Cont'd)

FIGURE		PAGE
11	Elementary excitation spectrum, $\epsilon(k)$, as function of ϕ_k for differ- ent ranges of α with $J_1 > 0$	74
12	Upper bounds for exact ground state energy per site for infinite chain with $J_1 > 0$, as function of α	81

Chapter I. Introduction

Much work has been done in the past fifty years on the development and solution, both exact and approximate, of various lattice model systems in one and higher dimensions. Nearest neighbour (nn), next nearest neighbour (nnn) and even higher order interactions have been used in the study of lattice systems. Models have been investigated for both zero and non-zero magnetic field (\mathcal{H}). Unfortunately, however, most of these model systems have not as yet been solved exactly and thus answers to many questions concerning them are either inconclusive or unknown.

Ising¹ solved the model named after him with nearest neighbour interactions and for all \mathcal{H} in the one-dimensional case in 1925. Onsager's famous solution² for the two-dimensional Ising model in zero field with nn interactions appeared in 1944; however, the three-dimensional problem is yet to be solved. The XY model has been solved only in one dimension^{3, 4}, and that only for nearest neighbour interactions with $\mathcal{H} = 0$. No exact solution has yet been found for the Heisenberg model in any dimension. A happy exception is the spherical model which has been solved⁵ in one, two and three dimensions with nn interactions for all \mathcal{H} ; however, the spherical model is not

very satisfying on various physical grounds.

Introducing next nearest neighbour and even higher order interactions produces a model which is closer to physical reality because there is no physical system whose statistical and thermodynamic properties can be completely explained by forces of finite magnitude which are so short-range that the only non-zero interaction energies are for nearest neighbour pairs of spins. Of course there are some physical systems which, to a good approximation, can be described, over a certain temperature range, by a lattice model using only nearest neighbour interactions. An example of this is the spin $\frac{1}{2}$ Ising model of a binary alloy.

The model systems mentioned, Ising, XY, Heisenberg and spherical, all involve a spin-spin bilinear exchange interaction. Work has been done on other more general interactions such as the spin-spin biquadratic exchange interaction^{6, 7}, the Dzyaloshinsky interaction⁸ and the dipole-dipole interaction⁹. It is even possible to postulate a tensor-tensor type of interaction. All of these more general interactions are more physically and experimentally relevant than spin-spin bilinear exchange interactions but, unfortunately, are also theoretically intractable at the present time.

In this Thesis we introduce next nearest neighbour interactions for two different one-dimensional lattice

models. For the spin $\frac{1}{2}$ Ising model in zero magnetic field the canonical partition function is found and its locus of zeros is then obtained for various ratios of the nnn to nn interaction energies. We also consider the zero field spin $\frac{1}{2}$ Heisenberg model. Repeating the work of Niemeijer¹⁰, we obtain an upper bound for the exact ground state energy per site at zero temperature for various different values of J_1 and J_2 , the nearest neighbour and next neighbour interaction energies, respectively. Part of the upper bound obtained by Niemeijer for the antiferromagnetic case, namely $J_1 > 0$, is shown to be incorrect.

It is a well known result that one-dimensional systems having short-range forces of finite magnitude cannot exhibit phase transitions with a transition temperature, T_c , greater than zero, though one can have $T_c > 0$ with long-range forces. Introducing nnn interactions into systems with long-range forces will alter the transition temperature. Bringing in next nearest interactions into our two models, even though it produces no change in T_c since the forces involved are of short-range, makes them more physically relevant and the resulting systems possess interesting features which make detailed investigation worthwhile.

Chapter II. One-Dimensional Spin $\frac{1}{2}$ Ising Model

1. Preliminaries

A useful method in discussing phase transitions is to investigate the distribution of zeros of the partition function. Physical and thermodynamic quantities can be determined once we find the locus of zeros and the distribution function on it. Suzuki¹¹ has derived the asymptotic form of the Helmholtz free energy and magnetization for the Ising model in terms of the distribution function of zeros in the complex fugacity plane. Even earlier, Yang and Lee¹², in discussing the phase transitions of lattice systems, proved that phase transitions occur when the locus of zeros of the partition function crosses the positive real axis of the complex fugacity plane with finite density of zeros (density is always zero on the real axis) as $N \rightarrow \infty$, where N is the total number of lattice sites (Yang-Lee Theorem). These are motivations for the general study of zeros of partition functions.

There are two specific reasons for looking at the zeros of the particular partition function examined in this chapter. First, Stephenson¹³ has shown for a certain range of nnn to nn interaction energies the existence of a disorder point, T_D , for which there is ferromagnetic

short-range order below this finite temperature and oscillatory exponential decay in the correlation above it. We want to see if the existence of a disorder point is reflected in the locus of zeros of the partition function.

Since the model we are investigating can be solved exactly, one can justifiably ask why study the zeros at all. The answer is that our calculations are being done as a trial run. Zeros for fixed ratios of J_2/J_1 have not been studied before; previous investigations fixed the ratio of J_1 and J_2 to the temperature, T . Jones¹⁴ proposed a picture of a phase transition using complex temperatures but the complex fugacity plane is better suited to the study of zeros of partition functions for fixed ratios of J_2 to J_1 . The second reason for studying the zeros of this simple one-dimensional model is, therefore, that it gives us an appreciation of the mathematical and computational intricacies involved in studying zeros from the viewpoint of fixed ratios of J_2/J_1 . Such an appreciation is necessary before tackling the same problem for more complicated one and two-dimensional systems.

In this section we consider a spin $\frac{1}{2}$ Ising linear chain with nearest and next nearest neighbour interactions present. Montroll¹⁵ has obtained the partition function of this system for the case where the magnetic field is zero by the method of an eigenvalue problem while Obokata and Oguchi¹⁶ got identical results by generalizing the

Bethe approximation. Oguchi¹⁷ found the partition function in the presence of a magnetic field by obtaining the eigenvalue equation of the transfer matrix for the system. The locus of zeros of the partition function for non-zero magnetic field was examined by Katsura and Ohminami¹⁸. In what follows, after obtaining the partition function by the transfer matrix method, we then investigate its locus of zeros in the case of zero magnetic field for different ratios of the next nearest neighbour to nearest neighbour interaction energies.

2. Zeros Of Partition Function

Consider an Ising linear chain with N lattice sites, having J_1 and J_2 as the interaction energies between nearest neighbour spins and next nearest neighbour spins, respectively. Let \mathcal{H} be the magnetic field and μ the magnetic moment associated with each spin. It is convenient to introduce a set of N dichotomic spin variables, $\{\sigma_i\}, i=1,2,\dots,N$, where at the i 'th lattice site,

$$\sigma_i = \begin{cases} +1, & \text{for spin up} \\ -1, & \text{for spin down} \end{cases}$$

For a particular configuration of spins $\{s\}$, the Hamiltonian is given by,

$$H = -J_1 \sum_{i=1}^{N-1} \sigma_i \sigma_{i+1} - J_2 \sum_{i=1}^{N-2} \sigma_i \sigma_{i+2} - \mu \mathcal{H} \sum_{i=1}^N \sigma_i \quad (2-1)$$

Introduce the notation,

$$K_1 = \frac{J_1}{kT} ; \quad K_2 = \frac{J_2}{kT} ; \quad L = \frac{\mu \mathcal{H}}{kT} \quad (2-2)$$

where k is Boltzmann's constant and T is the absolute temperature.

The canonical partition function for the system then is given by,

$$Z_N(K_1, K_2, L) = \sum_{\{s\}} \exp(-H/kT)$$

$$\begin{aligned}
= \prod_{\sigma_1=-1}^1 \dots \prod_{\sigma_N=-1}^1 \exp \left(K_1 \sum_{i=1}^{N-1} \sigma_i \sigma_{i+1} + K_2 \sum_{i=1}^{N-2} \sigma_i \sigma_{i+2} \right. \\
\left. + L \sum_{i=1}^N \sigma_i \right) \quad (2-3)
\end{aligned}$$

We consider the case $\mathcal{H} = 0$. Thus (2-3) becomes,

$$\begin{aligned}
Z_N(K_1, K_2, 0) = \prod_{\sigma_1=-1}^1 \dots \prod_{\sigma_N=-1}^1 \exp \left(K_1 \sum_{i=1}^{N-1} \sigma_i \sigma_{i+1} \right. \\
\left. + K_2 \sum_{i=1}^{N-2} \sigma_i \sigma_{i+2} \right) \quad (2-4)
\end{aligned}$$

We now quote Dobson's proof¹⁹ that,

$$Z_N(K_1, K_2, 0) = 2Z_{N-1}(K_2, 0, K_1) \quad (2-5)$$

Introduce a new set of N variables defined by,

$$\alpha_0 = \sigma_1 \quad (2-6)$$

$$\alpha_i = \sigma_i \sigma_{i+1} ; i=1, 2, \dots, N-1 \quad (2-7)$$

The inverse transformation is,

$$\sigma_i = \alpha_{i-1} \alpha_{i-2} \dots \alpha_1 \alpha_0 ; i=1, 2, \dots, N \quad (2-8)$$

The set of variables $\{\alpha_i\}, i=1, 2, \dots, N$ have possible values of ± 1 . Using (2-7),

$$\sigma_i \sigma_{i+2} = \alpha_i \alpha_{i+1} \quad (2-9)$$

Transforming the sums over the σ 's to the corresponding sums in terms of the new set of variables $\{\alpha_i\}$, our partition function (2-4) can be written,

$$Z_N(K_1, K_2, 0) = \sum_{\alpha_0=-1}^1 \sum_{\alpha_1=-1}^1 \dots \sum_{\alpha_{N-1}=-1}^1 \exp \left(K_1 \sum_{i=1}^{N-1} \alpha_i + K_2 \sum_{i=1}^{N-2} \alpha_i \alpha_{i+1} \right) \quad (2-10)$$

The sum over α_0 can be performed immediately to give a result in the dummy variables α_i which can be recognized as $2Z_{N-1}(K_2, 0, K_1)$, thus proving (2-5). The significance of Dobson's result is that it reduces the partition function of a linear chain with N spins having nn interactions J_1 and nnn interactions J_2 and magnetic field $\mathcal{H} = 0$, to twice the partition function of a linear chain with $N-1$ spins having nn interactions J_2 and no nnn interactions and magnetic field $\mathcal{H} = J_1/\mu$.

Changing the variables in a result given by Domb²⁰,

$$Z_{N-1}(K_2, 0, K_1) = \text{Tr}(V^{N-1}) \quad (2-11)$$

where V is the following 2×2 matrix,

$$V = \begin{pmatrix} e^{K_2+K_1} & e^{-K_2} \\ e^{-K_2} & e^{K_2-K_1} \end{pmatrix} \quad (2-12)$$

V is the transfer matrix of the system. Now, using a theorem from linear algebra,

$$\text{Tr}(V^{N-1}) = \lambda_+^{N-1} + \lambda_-^{N-1} \quad (2-13)$$

where λ_+ , λ_- are the two eigenvalues of the transfer matrix V. The characteristic, or secular, equation of V is,

$$\lambda^2 - 2\lambda e^{K_2} \cosh K_1 + (e^{2K_2} - e^{-2K_2}) = 0 \quad (2-14)$$

from which we obtain the two eigenvalues to be,

$$\lambda_{\pm} = e^{K_2} \cosh K_1 \pm (e^{2K_2} \sinh^2 K_1 + e^{-2K_2})^{1/2} \quad (2-15)$$

Thus, using (2-5),

$$Z_N(K_1, K_2, 0) = 2(\lambda_+^{N-1} + \lambda_-^{N-1}) \quad (2-16)$$

Equation (2-16) is the partition function we set out to evaluate. Its locus of zeros will now be examined.

Setting (2-16) to zero we obtain,

$$\lambda_+ = (-1)^{1/N-1} \lambda_- \quad (2-17)$$

Now,

$$(-1)^{1/N-1} = \exp\left(\frac{i(2k+1)\pi}{N-1}\right); \quad k=0,1,\dots,N-2 \quad (2-18)$$

The allowed values of k are restricted in (2-18) because we want only those $(N-1)$ st roots of (-1) which lie on the first Riemann sheet, namely between 0 and 2π radians in the complex number plane. Using (2-15) and (2-18), (2-17) becomes the following,

$$\tanh^2 K_1 + \frac{e^{-4K_2}}{\cosh^2 K_1} = -\tan^2 \phi_k \quad (2-19)$$

where,

$$\phi_k = \frac{\pi}{N-1} (k+\frac{1}{2}); \quad k=0,1,\dots,N-2 \quad (2-20)$$

The transcendental equation (2-19) gives the locus of zeros of the partition function (2-16).

For a particular system, J_1 and J_2 are fixed real numbers. Therefore we can define,

$$\lambda = \frac{J_2}{|J_1|}; \quad \lambda \text{ real}; \quad -\infty < \lambda < +\infty \quad (2-21)$$

Note that if we replace J_1 by $-J_1$, (2-19) remains unchanged. This means that the roots of (2-19) are not affected by a change in sign of the nearest neighbour interaction energy, J_1 . Therefore, without loss of

generality, we can set $J_1 = +1$. From (2-2),

$$K_1 = 1/kT \quad (2-22)$$

and,

$$\lambda = K_2/K_1 \quad (2-23)$$

or,

$$K_2 = \lambda K_1 = \lambda/kT \quad (2-24)$$

Using (2-24), (2-19) becomes,

$$\tanh^2 K_1 + \frac{e^{-4\lambda K_1}}{\cosh^2 K_1} = -\tan^2 \phi_k \quad (2-25)$$

We define the "fugacity", z , by,

$$z = e^{-2K_1} \quad (2-26)$$

Strictly speaking, z is not a fugacity but it is the quantity analogous to the fugacity in the grand canonical ensemble. In terms of z , equation (2-25) becomes,

$$\cos^2 \phi_k = \frac{(1+z)^2}{4z(1-z^{2\lambda})} ; z \neq 0, z^{2\lambda} \neq 1 \quad (2-27)$$

The roots of (2-27) are the zeros of the partition function (2-16). The imaginary part of (2-27) gives the locus of zeros and the real part gives a subsidiary condition that the zeros must satisfy. Numerical results of our calculations are given in the next section.

3. Numerical Results

To facilitate computations we introduce polar coordinates (ρ, ϕ) such that,

$$z = \rho e^{i\phi} \quad (2-28)$$

The advantage of using polar coordinates in discussing (2-27) is that, by so doing, we can be sure that we will obtain the roots on the first Riemann sheet and thus avoid the complications that come with multi-valuedness. Taking the complex conjugate of (2-27) we obtain,

$$\cos^2 \phi_k = \frac{(1+z^*)^2}{4z^*(1-z^{*2\lambda})} ; z^* \neq 0, z^{*2\lambda} \neq 1 \quad (2-29)$$

where z^* is the complex conjugate of z . Subtracting (2-27) and (2-29), then bringing the difference to a common denominator and using the four assumptions $z \neq 0$, $z^{2\lambda} \neq 1$, $z^* \neq 0$, $z^{*2\lambda} \neq 1$ we find that,

$$\begin{aligned} (1-\rho^2)\sin\phi - \rho^{2\lambda}\{\sin(2\lambda+1)\phi + 2\rho\sin 2\lambda\phi \\ + \rho^2\sin(2\lambda-1)\phi\} = 0; z \neq 0, z^{2\lambda} \neq 1 \end{aligned} \quad (2-30)$$

Equation (2-30) gives the locus of zeros in the complex fugacity plane.

Now, in equation (2-27) we multiply through by $4(1-z^{2\lambda})$; we can do this since we have assumed $z^{2\lambda} \neq 1$.

Equating real and imaginary parts we obtain the following two equations,

$$4\cos^2\phi_k = \frac{(\rho^{-1} + \rho)\cos\phi + 2}{1 - \rho^{2\lambda}\cos 2\lambda\phi} ; 1 - \rho^{2\lambda}\cos 2\lambda\phi \neq 0$$

$$, z^{2\lambda} \neq 1 \quad (2-31)$$

and,

$$4\cos^2\phi_k = \frac{(\rho^{-1} - \rho)\sin\phi}{\rho^{2\lambda}\sin 2\lambda\phi} ; \rho^{2\lambda}\sin 2\lambda\phi \neq 0, z^{2\lambda} \neq 1 \quad (2-32)$$

Equations (2-31) and (2-32) are two additional conditions that the roots of (2-27) must satisfy. Of the three equations (2-30), (2-31) and (2-32) only two are independent, as (2-30) can be obtained from the other two by the elimination of " $4\cos^2\phi_k$ ". By adding (2-31) and (2-32) an equation can be found which is directly related to the subsidiary condition mentioned at the end of Section 2. We will refer to (2-31) and (2-32) as two subsidiary conditions that the roots of (2-27) must satisfy, even though this terminology is not strictly valid.

We are interested in the case $N \rightarrow \infty$. Then, ϕ_k is continuous in the interval $0 \leq \phi_k \leq \pi$ and $\cos^2\phi_k$ is continuous in the interval $\{0, 1\}$, where the curly brackets indicate a closed interval, namely one in which the endpoints are included. Thus, in order for the subsidiary conditions (2-31) and (2-32) to be satisfied, the right hand sides

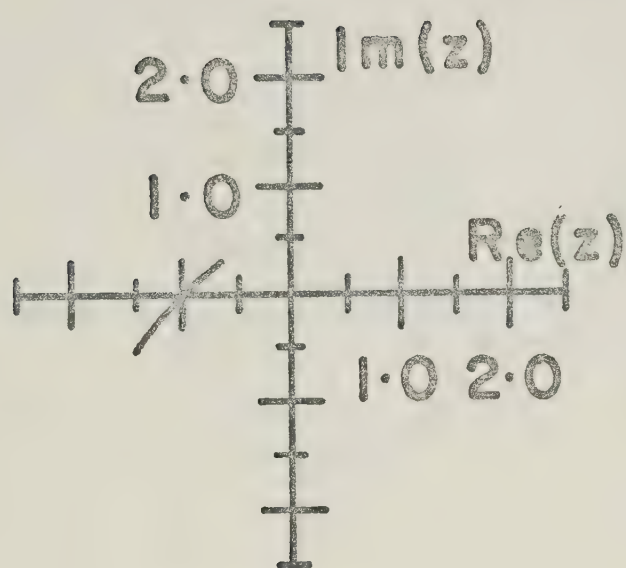
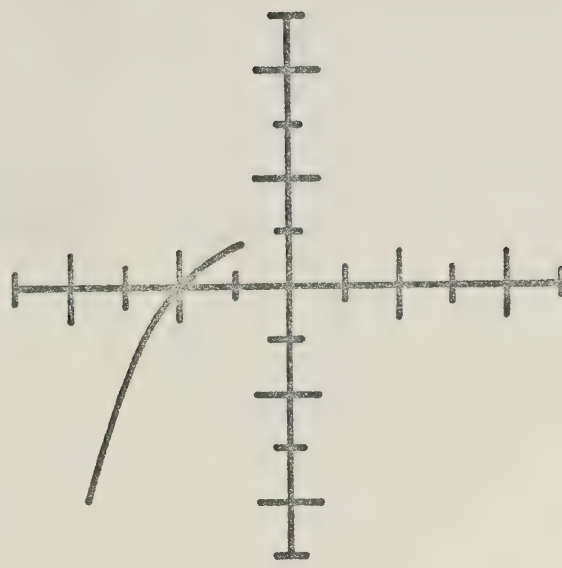
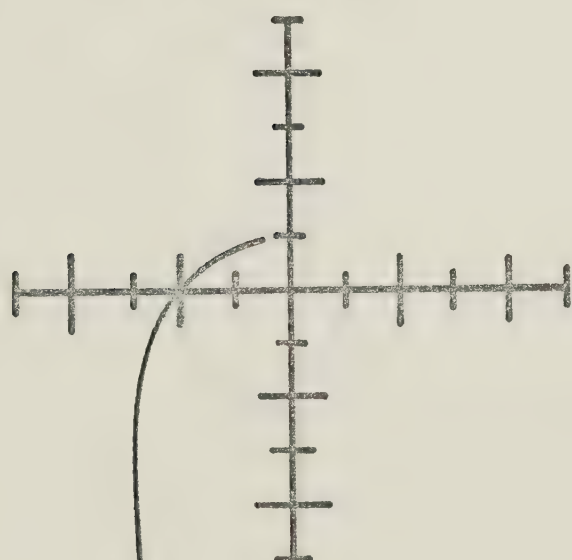
of the two equations must be in the interval $\{0,4\}$.

We have solved (2-30) numerically for various values of λ , subject to the constraints imposed by (2-31) and (2-32). The results for the locus of zeros of the partition function (2-16) in the complex z plane are given in Figures 1,2,3,4,5 and 6.

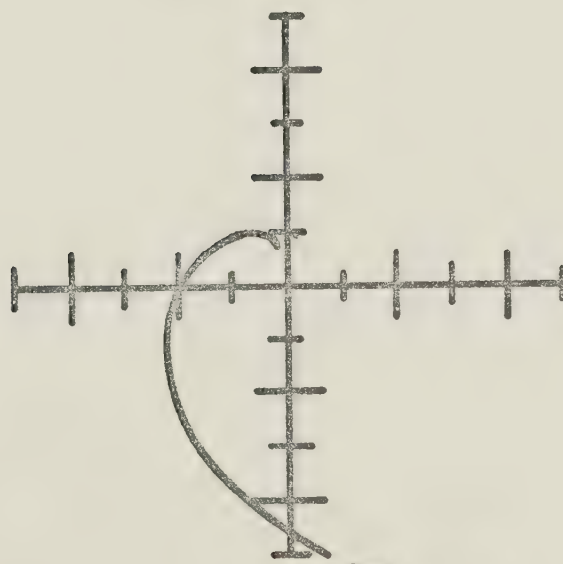
If in (2-27) we make the transformation $\lambda \rightarrow -\lambda'$, $z \rightarrow 1/z'$, we obtain the same equation in the primed variables as we had in the unprimed variables. This means that if the set of roots of (2-27) for $\lambda = \lambda_0$ is $\{z_0\}$, then the corresponding set of roots of (2-27) for $\lambda = -\lambda_0$ is $\{1/z_0\}$. Thus, to find the roots for $\lambda = -\lambda_0$ all we need to do is a complex inversion of the roots for $\lambda = \lambda_0$. Because of this symmetry in (2-27), we have not separately considered any negative values of λ ; positive values only have been investigated.

Figures 1,2,3,4,5 and 6: Locus of zeros of the partition function (2-16) in the complex fugacity plane for different values of λ . For all graphs horizontal axis gives real part of z and vertical axis the imaginary part. Scale for two axes is the same for all twenty-two graphs. If a particular branch of locus of zeros goes beyond the scale we have used, the point it approaches is given in terms of polar coordinates (ρ, ϕ) .

FIGURE 1

 $\lambda = 0.01$  $\lambda = 0.05$ $\lambda = 0.1$ 

$\rho \approx 4.6$
 $\phi \approx 253^\circ$

 $\lambda = 0.2$ 

$\rho \approx 14$
 $\phi \approx 312^\circ$

FIGURE 2

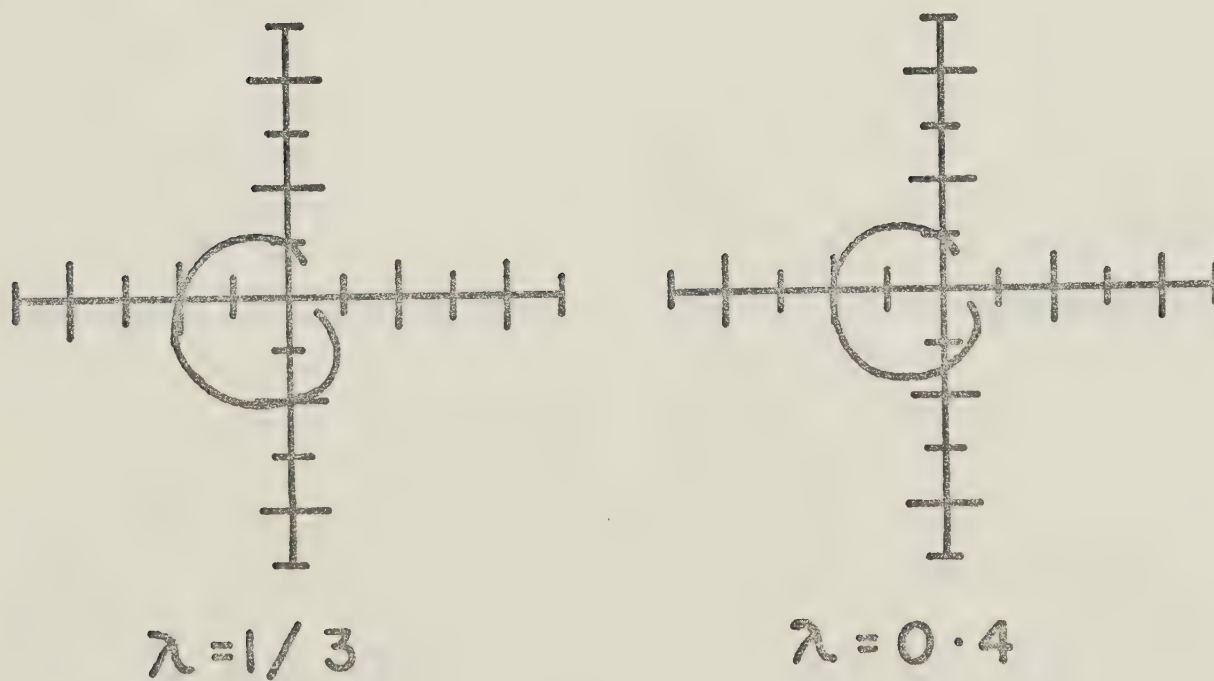
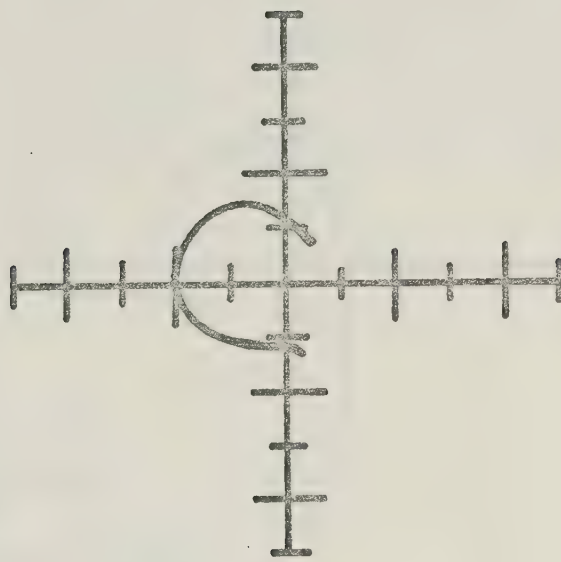


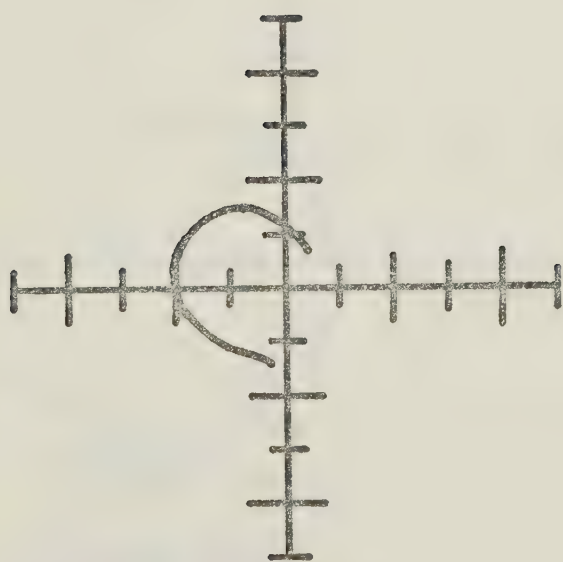
FIGURE 3



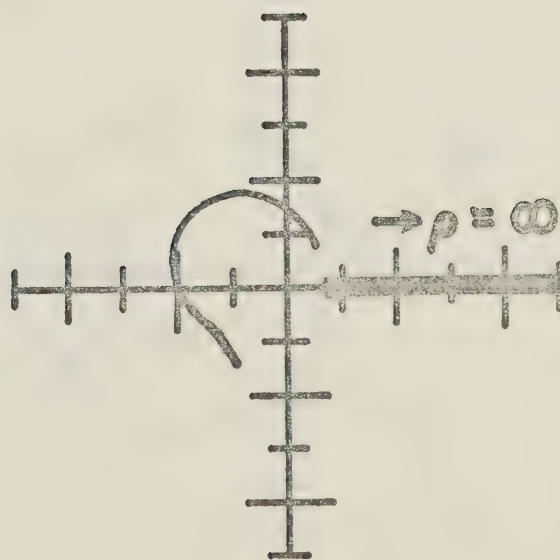
$$\lambda = 0.5$$



$$\lambda = 0.6$$



$$\lambda = 2/3$$



$$\lambda = 0.75$$

FIGURE 4

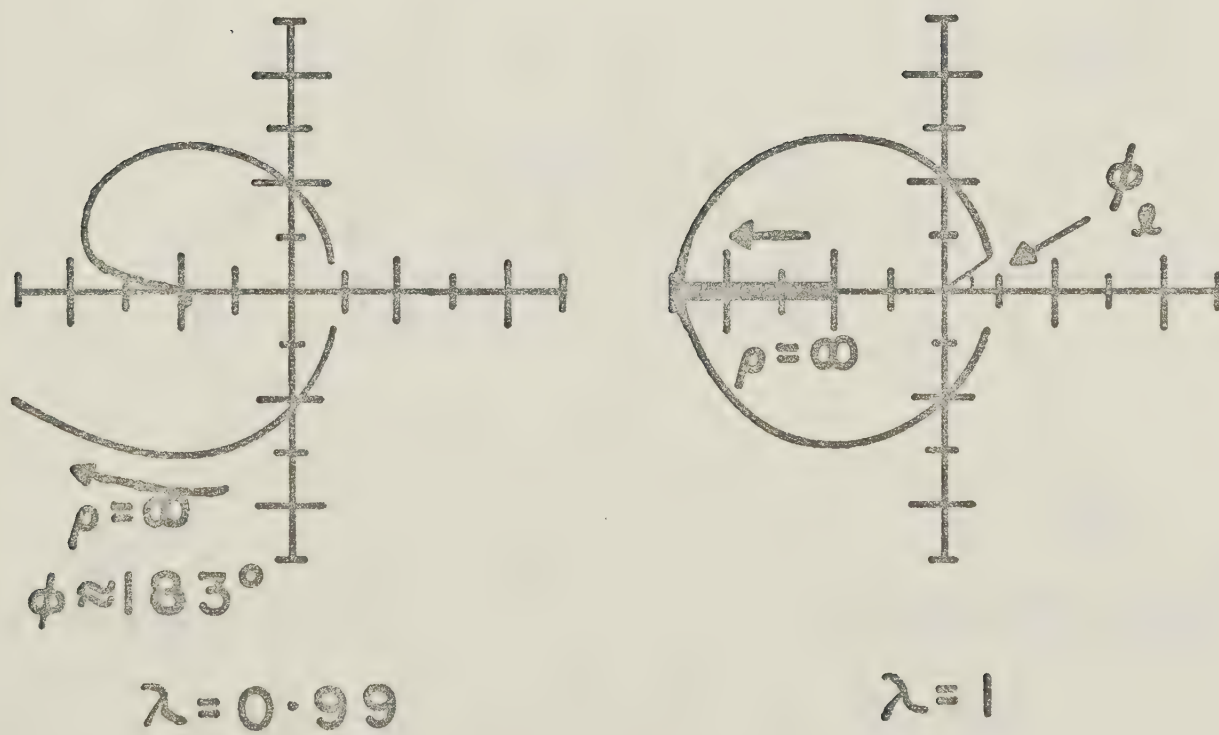
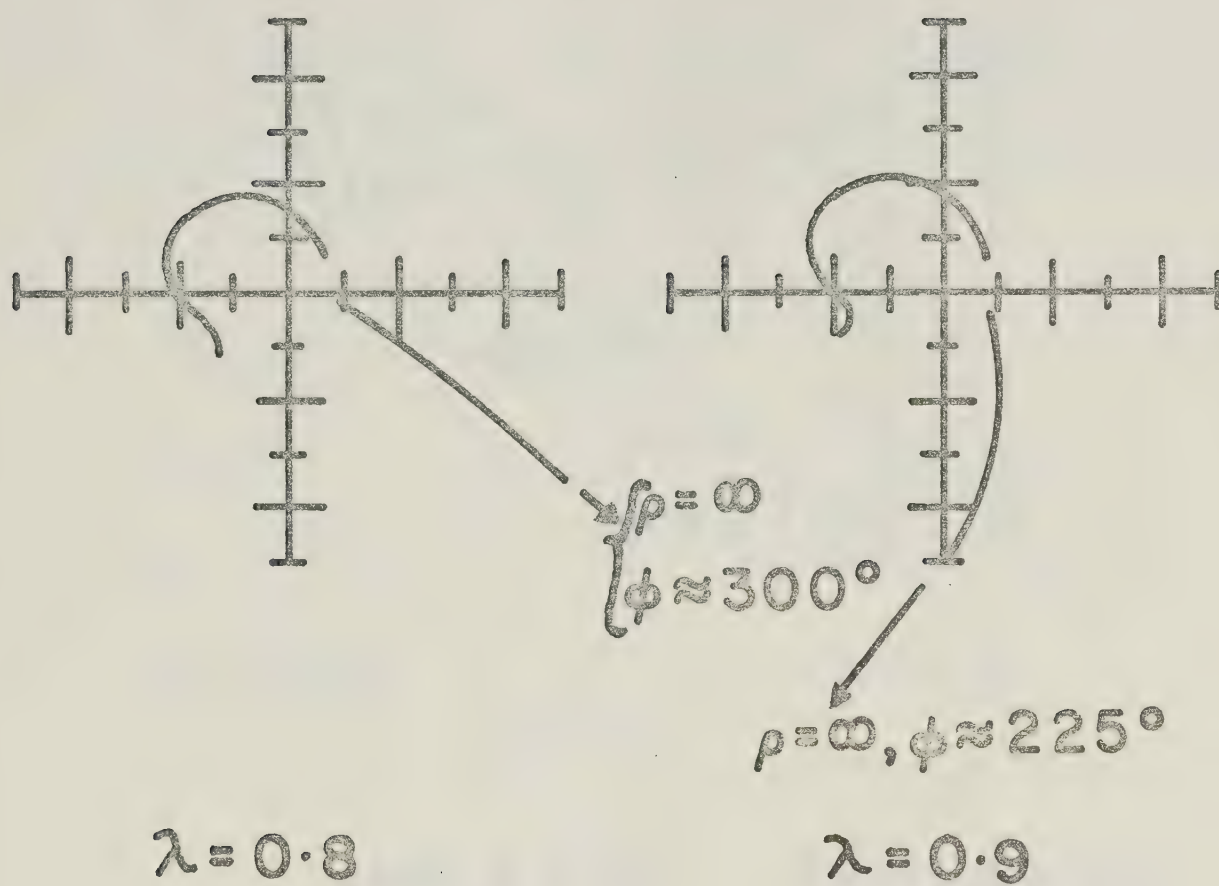


FIGURE 5

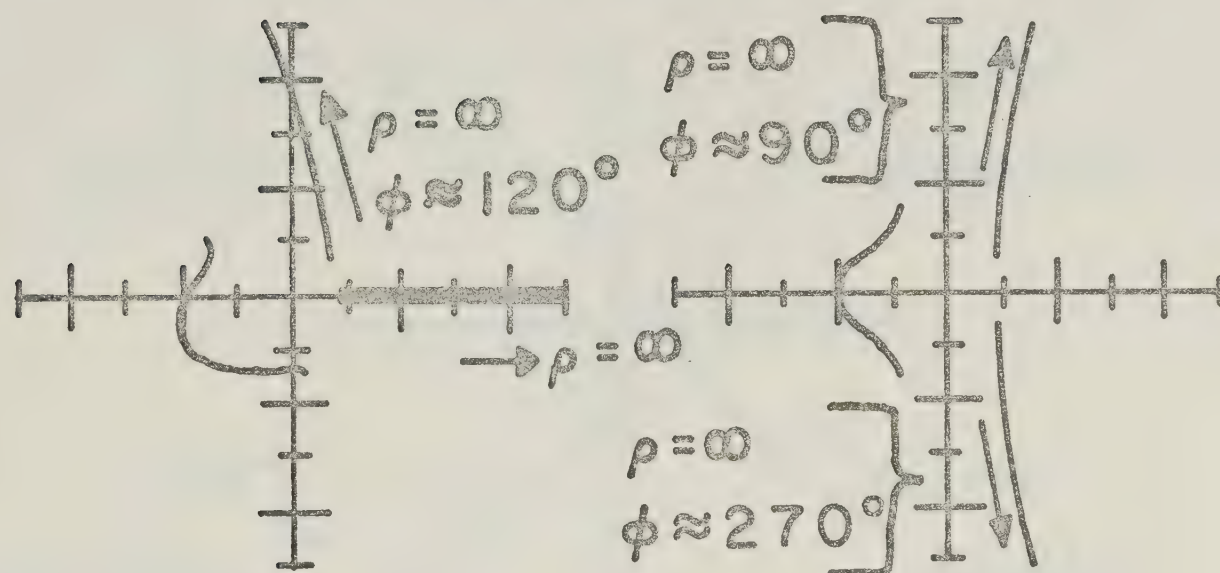
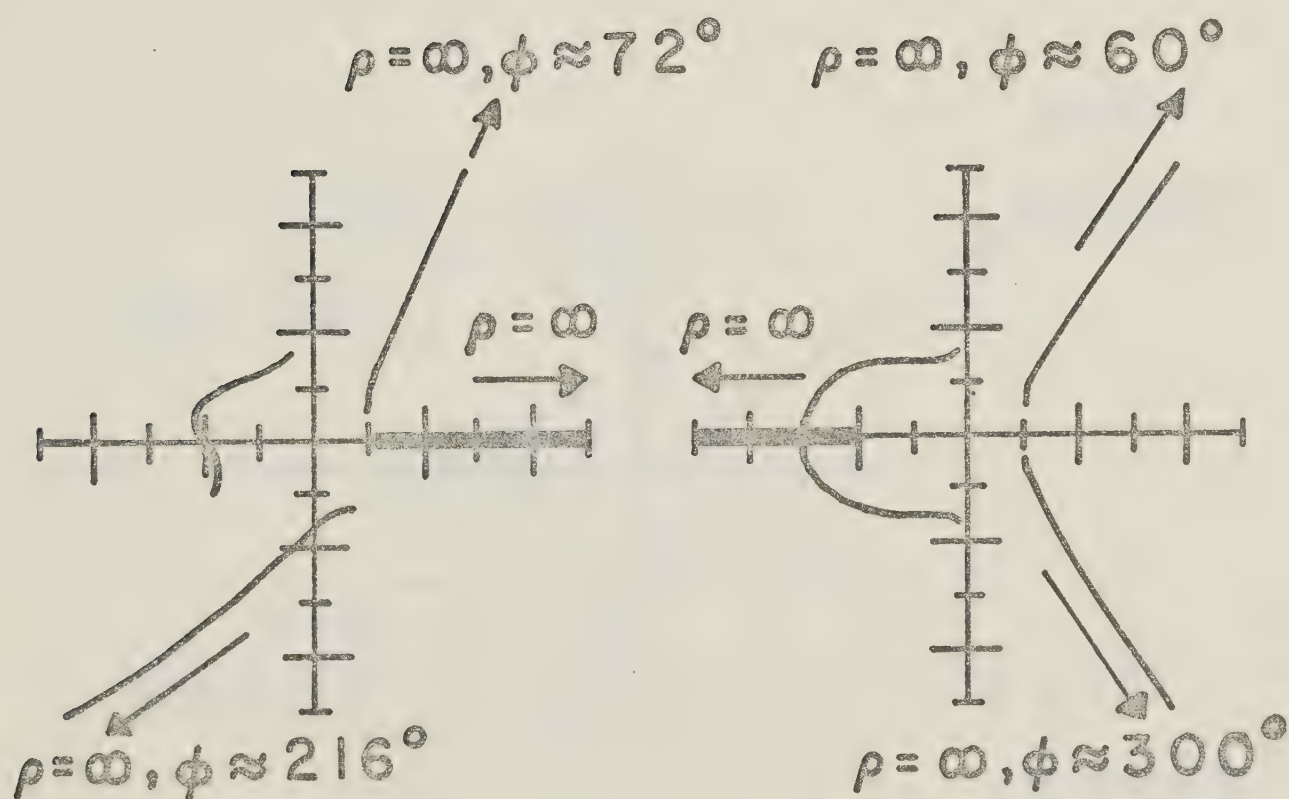
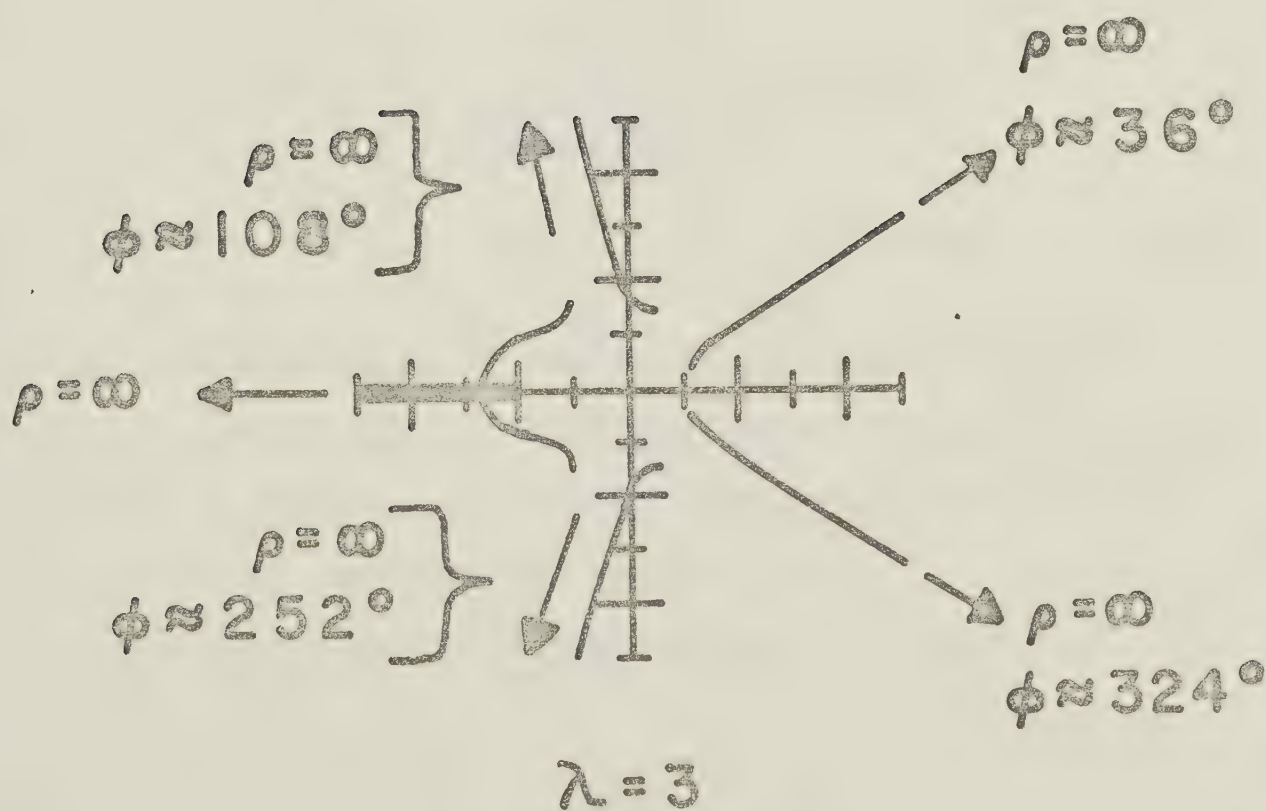
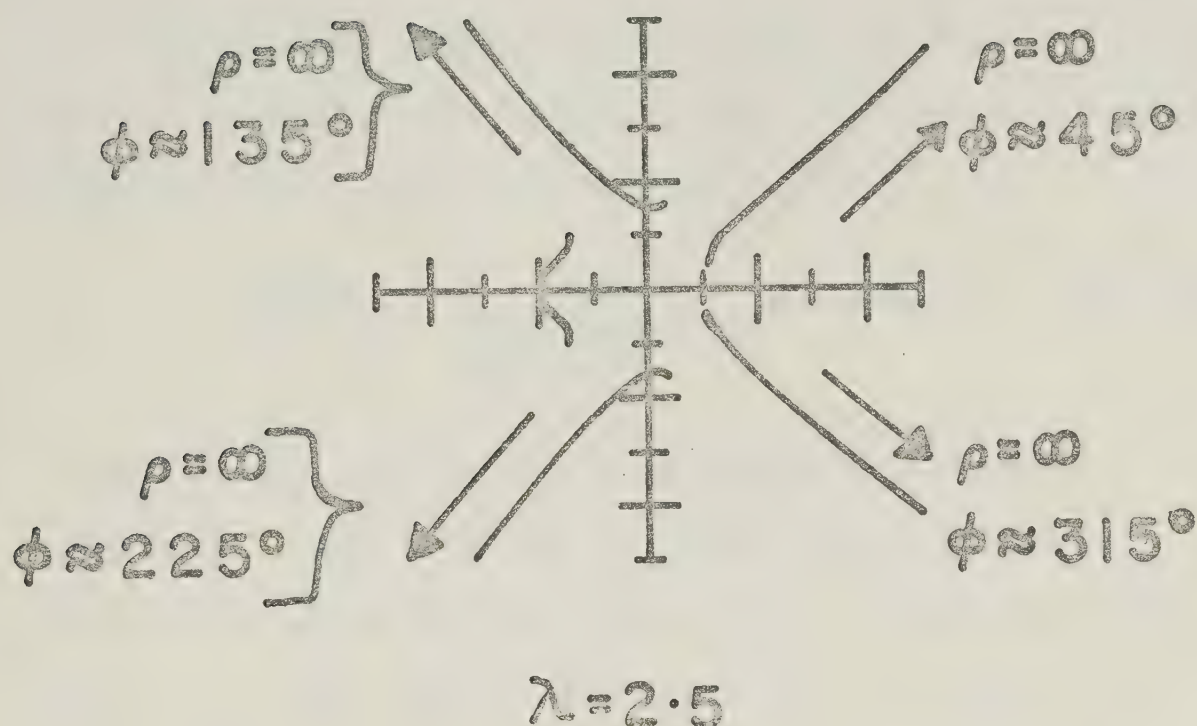
 $\lambda = 1.25$ $\lambda = 1.5$  $\lambda = 1.75$ $\lambda = 2$

FIGURE 6



4. Discussion Of Numerical Results

A. Properties Of Solutions - The General Case

We now work with equation (2-27) to obtain some exact results by analytical means. First we investigate solutions for $\phi = 0$. (2-27) becomes,

$$\cos^2 \phi_k = \frac{(1+\rho)^2}{4\rho(1-\rho^{2\lambda})} ; \rho \neq 0, \rho^{2\lambda} \neq 1 \quad (2-33)$$

We want those real positive values of ρ for which $0 \leq \cos^2 \phi_k \leq 1$. Using (2-33) we find that there are no values of ρ which satisfy both of the inequalities simultaneously. This means that there are no solutions of (2-27) for $\phi = 0$.

For $\phi = \pi$,

$$\cos^2 \phi_k = \frac{(1-\rho)^2}{-4\rho(1-\rho^{2\lambda}e^{2i\lambda\pi})} ; \rho \neq 0$$

$$, \rho^{2\lambda}e^{2i\lambda\pi} \neq 1 \quad (2-34)$$

Using the continuity of $\cos^2 \phi_k$ in the closed interval $\{0,1\}$ in conjunction with (2-34) we can examine the three cases 2λ an even or odd integer and $2\lambda \neq \text{integer}$. We get the following as solutions for $\phi = \pi$:

a). $1 < \rho < \infty$, for $2\lambda = \text{even integer } (\lambda=1,2,3,\dots)$.

b). $\rho = 1$, otherwise.

Our numerical results, as given in Figures 1 through 6, bear this out.

Next we look at the situation when $\phi = 2\pi$. Equation (2-27) gives,

$$\cos^2 \phi_k = \frac{(1+\rho)^2}{4\rho(1-\rho^{2\lambda} e^{4i\lambda\pi})} ; \rho \neq 0, \rho^{2\lambda} e^{4i\lambda\pi} \neq 1 \quad (2-35)$$

Again we want those real positive values of ρ for which $0 \leq \cos^2 \phi_k \leq 1$. For 4λ an even integer and $4\lambda \neq \text{integer}$, (2-35) has no valid solutions; however, for 4λ an odd integer ($\lambda = 1/4, 3/4, 5/4, \dots$), there is a ρ interval for which the requirement on $\cos^2 \phi_k$ is met. The numerical values of the first four intervals are the following:

a). $0.263805 \leq \rho \leq 19.7057$, for $\lambda = 1/4$.

b). $\rho \geq 0.387849$, for $\lambda = 3/4$.

c). $\rho \geq 0.468800$, for $\lambda = 5/4$.

d). $\rho \geq 0.526912$, for $\lambda = 7/4$.

Intervals for $\lambda = 9/4, 11/4, \dots$ can be worked out also.

Thus, solutions for $\phi = 2\pi$ exist for odd positive quarter integer values of λ and the solutions are either finite ($\lambda = 1/4$) or semi-infinite ($\lambda = 3/4, 5/4, \dots$) intervals along the positive real fugacity axis. These solutions are shown for the appropriate cases in Figures 1-6.

We can also examine solutions of (2-27) for $\rho = 1$, for which we have,

$$\cos^2 \phi_k = \frac{1+e^{i\phi}}{4e^{i\phi}(1-e^{2i\lambda\phi})} ; e^{i\phi} \neq 0, e^{2i\lambda\phi} \neq 1 \quad (2-36)$$

Simplifying (2-36), then separating real and imaginary parts we obtain,

$$\frac{1+\cos\phi}{4} = \cos^2 \phi_k ; e^{i\phi} \neq 0, e^{2i\lambda\phi} \neq 1 \quad (2-37)$$

and,

$$\frac{(1+\cos\phi)\sin 2\lambda\phi}{4(1-\cos 2\lambda\phi)} = 0 ; e^{i\phi} \neq 0, e^{2i\lambda\phi} \neq 1 \quad (2-38)$$

We want only those roots of (2-38) which satisfy the constraint imposed by (2-37). For the first Riemann sheet we consider only those values of ϕ in the closed interval $\{0, 2\pi\}$. For all values of ϕ in this interval, $\cos^2 \phi_k$ given by (2-37) satisfies $0 \leq \cos^2 \phi_k \leq 1$. Thus the roots of (2-38) are the solutions of (2-27) for $\rho = 1$. We find the solutions for $\rho = 1$ to be the following:

- a). $\phi = \pi$, for $\lambda \neq \text{integer } (\lambda \neq 1, 2, 3, \dots)$.
- b). $\phi = \frac{m\pi}{2\lambda} ; m=0, 1, 2, \dots, [4\lambda]$, for $\frac{m}{2\lambda} \neq \text{integer}$ and for m odd.
- c). $\phi = 2\pi$, for $4\lambda = \text{odd integer } (\lambda=1/4, 3/4, 5/4, \dots)$.

where we have defined,

$$[x] \equiv \begin{cases} \text{greatest integer contained in} \\ x, \text{ for } x \geq 0 \\ 0, \text{ otherwise} \end{cases} \quad (2-39)$$

The first and third types of solutions for $\rho = 1$ are

consistent with the solutions we have already found for $\phi = \pi$ and $\phi = 2\pi$, respectively. As an example let us consider $\lambda = 1.25$. Two solutions of (2-27) are $(\rho, \phi) = (1, \pi)$ and $(\rho, \phi) = (1, 2\pi)$. Since $[4\lambda] = 5$, the allowed odd values of m are $m = 1, 3, 5$. However, for $m = 5$, $\frac{m}{2\lambda} = 2$, an integer, so $m = 5$ must also be excluded. Thus the other two solutions of (2-27) for $\rho = 1$, $\lambda = 1.25$ are, from $m = 1$ and 3 , $(\rho, \phi) = (1, \frac{2}{5}\pi), (1, \frac{6}{5}\pi)$. These four solution points can be seen in the graph for $\lambda = 1.25$ in Figure 5.

Next, we look for large ρ solutions of (2-27). For solutions where z is large in magnitude,

$$\cos^2 \phi_k \approx -\frac{1}{4z^{2\lambda-1}} ; z \neq 0, z^{2\lambda} \neq 1 \quad (2-40)$$

Since $\cos^2 \phi_k$ must satisfy $0 \leq \cos^2 \phi_k \leq 1$, this means that large ρ solutions are possible only if $2\lambda-1 > 0$, that is $\lambda > \frac{1}{2}$. Equating real and imaginary parts in (2-40),

$$\frac{\cos(2\lambda-1)\phi}{-4\rho^{2\lambda-1}} = \cos^2 \phi_k ; \rho e^{i\phi} \neq 0, \rho^{2\lambda} e^{2i\lambda\phi} \neq 1 \quad (2-41)$$

and,

$$\frac{\sin(2\lambda-1)\phi}{4\rho^{2\lambda-1}} = 0 ; \rho e^{i\phi} \neq 0, \rho^{2\lambda} e^{2i\lambda\phi} \neq 1 \quad (2-42)$$

Solving (2-42) subject to the constraint imposed by (2-41) and using the fact that ϕ is restricted to the first Rie-

mann sheet, $0 \leq \phi \leq 2\pi$, we arrive at the result that (2-27) has large ρ solutions, namely $\rho \rightarrow \infty$, for $\phi = n\pi/(2\lambda-1)$, where $n = 1, 3, 5, \dots, [4\lambda-2]$ if $[4\lambda-2]$ is odd and $n = 1, 3, 5, \dots, [4\lambda-2]-1$ if $[4\lambda-2]$ is even. From this it is easy to show that the number of large ρ solutions in the closed interval $\{0, 2\pi\}$ is $[2\lambda-\frac{1}{2}]$ if $[4\lambda-2]$ is odd and $[2\lambda-1]$ if $[4\lambda-2]$ is even. Thus there are large ρ solutions of (2-27) for all values of λ satisfying $2\lambda-\frac{1}{2} \geq 1$, namely for all $\lambda \geq 3/4$; our numerical results, Figures 1-6, bear this out. Let us look at the case $\lambda = 3$ as an example. $[4\lambda-2]$ is even so there should be $[2\lambda-1] = 5$ large ρ solutions, and there are. They should occur at $\phi = n\pi/5$, $n = 1, 3, 5, 7, 9$, that is at $\phi = \pi/5, 3\pi/5, \pi, 7\pi/5, 9\pi/5$. From the graph for $\lambda = 3$ in Figure 6, large ρ solutions do exist for these five values of ϕ .

We note another interesting feature of (2-27). If $(\rho, \phi) = (\rho_1, \pi - \phi_1)$ is a solution, then $(\rho, \phi) = (\rho_1, \pi + \phi_1)$ is also a solution when $\lambda = n/2$; $n = 0, 1, 2, \dots$. This symmetry is reflected in the appropriate plots in Figures 1-6. For no other values of λ other than integer and half-integer values are the loci of zeros symmetric about $\phi = \pi$.

Finally, we give a qualitative description of the behaviour of the locus of zeros for increasing λ ; this is in reference to the graphs in Figures 1-6. For λ small and increasing the locus expands out from the point $z = -1$. The branch in the upper half of the complex z plane

bends toward the $\phi = 0$ axis while the branch in the lower half bends counterclockwise and approaches the positive real axis ($\phi = 2\pi$); it reaches it when $\lambda = 0.25$. Also for this value of λ , there is a finite solution interval on the positive real fugacity axis. For $\lambda > 0.25$, the locus assumes a roughly circular form with a bulge which is the departure from circularity being below the real axis. At $\lambda = 0.5$, the locus looks like a circular arc. For $\lambda > 0.5$, the bulge appears again, this time above the real axis and travels clockwise with increasing λ . At $\lambda = 0.75$, our first large ρ solution appears at $\phi = 2\pi$ from the second Riemann sheet. It rotates clockwise and reaches the negative real axis ($\phi = \pi$) when $\lambda = 1$. For $\lambda > 0.75$, the bulge changes direction and again approaches $\phi = \pi$; at $\lambda = 1$, this branch of the locus again looks like a circular arc. For $\lambda > 1$, the bulge moves below the real axis and the first large ρ solution continues to rotate clockwise. At $\lambda = 1.25$, the second large ρ solution appears at $\phi = 2\pi$ and begins to travel clockwise as λ increases. At $\lambda = 1.5$, the bulge again crosses the real z axis: The third large ρ solution enters the first Riemann sheet at $\phi = 2\pi$ when $\lambda = 1.75$ and also moves clockwise for increasing λ . The bulge crosses the real axis at $\lambda = 2$ again, at which point the second large ρ solution has reached $\phi = \pi$. As λ increases, we see that we get additional large ρ solutions appearing at $\phi = 2\pi$ each time we reach an odd quarter-integer value of λ ; these large ρ solutions then

rotate clockwise with further increase in λ . One large ρ solution crosses the negative real axis whenever λ takes on an integer value. More and more branches of the locus of zeros appear in the first Riemann sheet as λ gets larger.

B. Exactly Soluble Cases

For certain values of λ equation (2-27) can be solved exactly by analytic means. For $\lambda = \frac{1}{2}$,

$$\cos^2 \phi_k = \frac{(1+z)^2}{4z(1-z)} ; z \neq 0, z \neq 1 \quad (2-43)$$

This can be expressed as a quadratic equation whose solution is,

$$z = \frac{1}{2} - \frac{3}{2(1+4\cos^2 \phi_k)} \pm iB \quad (2-44a)$$

where,

$$B = \frac{2\cos \phi_k (2 - \cos^2 \phi_k)^{\frac{1}{2}}}{1 + 4\cos^2 \phi_k} \quad (2-44b)$$

We introduce coordinates (r,s) defined by,

$$z = r + is \quad (2-45)$$

(2-44a) can then be put in the form,

$$(r + 1/3)^2 + s^2 = 4/9 \quad (2-46)$$

(2-46) is the equation of a circle with center at $(r,s) = (-1/3, 0)$ and having radius $2/3$. Thus, the locus of zeros in the complex fugacity plane for $\lambda = \frac{1}{2}$ is a circular arc given by that part of the circle defined by (2-46) for which $0 \leq \cos^2 \phi_k \leq 1$. The endpoints of the arc are at $(r,s) =$

$(1/5, \pm 2/5)$ and the angle $\phi_c = \sin^{-1}(2/\sqrt{5}) \approx 63.3^\circ$ (see Figure 3).

Next we consider $\lambda = 1$ for which,

$$\cos^2 \phi_k = \frac{1+z}{4z(1-z)} ; z \neq 0, z^2 \neq 1 \quad (2-47)$$

Expressing this as a quadratic equation we obtain as the solution,

$$z = \begin{cases} (C_1 \pm C_2^{1/2})/C_3 ; 0 \leq 4\cos^2 \phi_k < 3-2\sqrt{2} \\ (C_1 \pm i(-C_2)^{1/2})/C_3 ; 3-2\sqrt{2} < 4\cos^2 \phi_k \leq 4 \\ -1-\sqrt{2} ; 4\cos^2 \phi_k = 3-2\sqrt{2} \end{cases} \quad (2-48a)$$

where,

$$C_1 = 4\cos^2 \phi_k - 1 \quad (2-48b)$$

$$C_2 = (1-4\cos^2 \phi_k)^2 - 16\cos^2 \phi_k \quad (2-48c)$$

$$C_3 = 8\cos^2 \phi_k \quad (2-48d)$$

For $0 \leq 4\cos^2 \phi_k \leq 3-2\sqrt{2}$, the locus of zeros given by (2-48a) is a straight line on the negative real z axis such that $-\infty \leq r \leq -1$. For $3-2\sqrt{2} < 4\cos^2 \phi_k \leq 4$, we use (2-45) to express (2-48a) as,

$$(r+1)^2 + s^2 = 2 \quad (2-49)$$

(2-49) is the equation of a circle with center at $(r,s) =$

$(-1,0)$ and having radius $\sqrt{2}$. Thus, the locus of zeros in the complex fugacity plane for $\lambda = 1$ is a straight line on the negative real axis such that $-\infty \leq r \leq -1$ and a circular arc given by that part of the circle defined by (2-49) for which $3-2\sqrt{2} < 4\cos^2\phi_k \leq 4$. The endpoints of the arc are located at $(r,s) = (3/8, \pm\sqrt{7}/8)$ and the angle $\phi_g = \sin^{-1}(\sqrt{7}/4) \approx 41.4^\circ$ (see Figure 4).

It is also possible to obtain the exact solution of (2-27) for $\lambda = 1/4, 3/2$ and 2 . However, these three cases were not done as they involved the algebraic solution of quartic equations.

C. Other Special Cases

As mentioned in Section 1 on Preliminaries, Stephenson¹³ has shown for $-\frac{1}{2} < \lambda < 0$ the existence of a disorder point, T_D . If this existence did peculiar things to the loci of zeros of the partition function (2-16) for $-\frac{1}{2} < \lambda < 0$, then these peculiarities would be reflected in the loci of zeros for $0 < \lambda < \frac{1}{2}$, since one set of loci can be obtained from the other by a simple complex inversion in the complex fugacity plane. This symmetry of equation (2-27) has been discussed in Section 3 on Numerical Results. However, the loci for $0 < \lambda < \frac{1}{2}$ are not unusual in comparison with those for $\lambda \geq \frac{1}{2}$, as can be seen in Figures 1-6. Indeed, as we have described in Subsection A of this section, there is a smooth and progressive evolution of the locus of zeros with increasing λ . We thus see that the existence of a disorder point does not appear to have any unusual effects on the locus of zeros.

The case $\lambda = -\frac{1}{2}$ has a special significance. In the previous subsection, we solved $\lambda = \frac{1}{2}$ exactly and showed the locus of zeros to be a circular arc; thus, $\lambda = -\frac{1}{2}$ also gives a circular arc. We have $J_2 = -\frac{1}{2}|J_1|$. Using Dobson's result, equation (2-5), the variables for the corresponding nn chain with interaction $J (= J_2)$ and magnetic field $\mathcal{H} (= J_1/\mu)$ now satisfy $2|J| = \mu\mathcal{H}$. This is the condition for the critical magnetic field of an antiferro-

magnetic chain²⁰.

Finally, $\lambda = 0.25$ also seems to be a special case due to the presence of the finite solution interval at $\phi = 2\pi$ (see Figure 2). Since large ρ solutions are not possible until $\lambda \geq 3/4$, the reason for the appearance of this interval is that it arises because of the mathematics of the problem. The interval has no physical significance since $\phi = 2\pi$ is not physical. For this same reason solutions at $\phi = 2\pi$ for all λ are non-physical; they come purely from the mathematics.

Chapter III. One-Dimensional Spin $\frac{1}{2}$ Heisenberg Model

1. Preliminaries

The Heisenberg model, of which the Ising and XY models are special cases, is an interesting theoretical model to study because it involves all three spin components. For this reason it is also mathematically more complex. For an infinite linear chain of spins interacting with nearest neighbours only via a Heisenberg interaction, the exact energy eigenstates were found by Bethe²¹ and Hulthén²² later obtained the exact ground state energy for the antiferromagnetic case. Orbach²³ derived the ground state wavefunctions for the linear antiferromagnetic Heisenberg chain. The exact partition function and wavefunctions for non-zero temperature, however, are not yet known.

If next nearest neighbour interactions are also taken into account, the rigorous ground state energy has not yet been obtained by analytical means. Various approximate methods have been used. In the classical approximation spin vectors in the Hamiltonian are replaced by classical vectors; Kaplan²⁴ is one of those who have used this classical picture to examine the ground state and its properties. In this approximation one expresses the energy for an N spin linear chain as,

$$E = J_1 \sum_{i=1}^N S^2 \cos \theta_{i,i+1} + J_2 \sum_{i=1}^N S^2 \cos \theta_{i,i+2} \quad (3-1-1)$$

where S is the length of the classical spin vector, $\theta_{i,i+1}$ the angle between spins at sites i and $i+1$, $\theta_{i,i+2}$ the angle between spins at sites i and $i+2$ and J_1, J_2 are the nearest and next nearest neighbour interaction energies, respectively. The ground state energy per spin then is,

$$E_0 = \begin{cases} -S^2 \left(\frac{J_1^2}{8J_2} + J_2 \right) , & \text{if } J_2 > 0 \text{ and } |J_1| \leq 4|J_2| \\ S^2 (\pm J_1 + J_2) , & \text{otherwise} \end{cases} \quad (3-1-2)$$

where the "+" sign refers to ferromagnetism ($J_1 < 0$) and the "-" sign to antiferromagnetism ($J_1 > 0$). For $J_2 > 0$ and $|J_1| \leq 4|J_2|$ the classical spin chain has a spiral structure at $T = 0$. The ground state energy has a kink at $J_2 = \frac{1}{4}J_1$ when plotted as a function of J_2 for a fixed value of J_1 .

Yoshida and Miwa²⁵ and recently Ono²⁶ have employed spin-wave approximations to discuss the problem of obtaining the ground state energy with both nn and nnn interactions present. Majumdar and Ghosh²⁷ determined some properties of finite linear Heisenberg chains and from these derived upper and lower bounds for the ground state energy per spin as the number of spins in the chain tended to infinity. Variational methods have given good agreement with the known exact results of Bethe for the case of nn interactions only, so Niemeijer¹⁰ has made use of a variational technique for the case where nnn interac-

tions are also present.

In this chapter we check Niemeijer's calculations on the one-dimensional spin $\frac{1}{2}$ Heisenberg model in zero field having both nn and nnn interactions present. An upper bound for the exact ground state energy per site at zero temperature is obtained for various different values of the two interaction energies. Part of the upper bound derived by Niemeijer for the antiferromagnetic nearest neighbour case is shown to be wrong and the correct upper bound, which is an improvement on his results, is found. Letting α be the ratio of nnn to nn interaction strengths, we also obtain the asymptote for the energy upper bound for ferromagnetic nearest neighbour interactions having large negative α and for antiferromagnetic nearest neighbour interactions having large positive α .

2. Calculation Of Single-Particle Energy, $\epsilon(k)$

We begin our review of Niemeijer's work¹⁰ by considering a one-dimensional chain with N lattice sites having J_1 and J_2 as the nearest neighbour and next nearest neighbour interaction energies, respectively. In zero magnetic field and for Heisenberg type interactions the Hamiltonian for the system is,

$$H = J_1 \sum_{j=1}^N \vec{S}_j \cdot \vec{S}_{j+1} + J_2 \sum_{j=1}^N \vec{S}_j \cdot \vec{S}_{j+2} \quad (3-1)$$

where S_j^i is the i component of the spin operator at the j 'th site and where cyclic boundary conditions have been taken, namely $\vec{S}_{N+1} = \vec{S}_1$ and $\vec{S}_{N+2} = \vec{S}_2$. For the quantum mechanical spin $\frac{1}{2}$ case, the S 's are the Pauli spin matrices. Even with $J_2 = 0$ this is a difficult problem for only the ground state and a few excited states are known^{21,22}. For our problem we use a temperature dependent Hartree-Fock approximation and we express the Hamiltonian (3-1) in terms of Fermi operators, which can be done because we are considering the spin $\frac{1}{2}$ case.

First we perform the transformation,

$$S_j^x = \frac{1}{2}(a_j^\dagger + a_j) \quad (3-2a)$$

$$S_j^y = \frac{1}{2i}(a_j^\dagger - a_j) \quad (3-2b)$$

$$S_j^z = a_j^\dagger a_j - \frac{1}{2} \quad (3-2c)$$

in terms of which (3-1) becomes,

$$\begin{aligned} H = \sum_{j=1}^N \{ & \frac{1}{2}(J_1 a_j a_{j+1}^\dagger + J_2 a_j a_{j+2}^\dagger + J_1 a_j^\dagger a_{j+1} \\ & + J_2 a_j^\dagger a_{j+2}) + J_1 a_j^\dagger a_j a_{j+1}^\dagger a_{j+1} \\ & + J_2 a_j^\dagger a_j a_{j+2}^\dagger a_{j+2} - \frac{1}{2}(J_1 a_{j+1}^\dagger a_{j+1} \\ & + J_2 a_{j+2}^\dagger a_{j+2}) - \frac{1}{2}(J_1 + J_2) a_j^\dagger a_j \\ & + \frac{1}{4}J_1 + \frac{1}{4}J_2 \} \end{aligned} \quad (3-3)$$

where the symbol "+" after an operator refers to the Hermitian conjugate of that operator. For the ferromagnetic ground state we can take either all spins up or all spins down; it does not really matter which, as long as consistency is retained throughout. In this chapter we will consider the ground state to be all spins down. The physical significance of a_j^\dagger is that it is a creation operator. Applied to the j 'th site in its ground state it creates an up spin, which is an excitation of the ground state. Similarly, a_j is an annihilation operator because, applied to an up spin at the j 'th site (excited state), it annihilates the up spin and leaves a down spin (ground state). The expectation value of the

number operator $a_j^\dagger a_j$ gives the occupation number of the excited state at the j 'th site.

We make the further transformation,

$$\begin{aligned} a_j &= \exp\{-\pi i \sum_{k=1}^{j-1} c_k^\dagger c_k\} c_j \\ a_j^\dagger &= c_j^\dagger \exp\{\pi i \sum_{k=1}^{j-1} c_k^\dagger c_k\} \end{aligned} \quad (3-4)$$

Equation (3-3) is then written as,

$$\begin{aligned} H &= \sum_{j=1}^N \{ \frac{1}{2} (J_1 c_j^\dagger c_{j+1} + J_2 c_j^\dagger c_{j+2} + \text{h.c.}) \\ &\quad + J_1 c_j^\dagger c_j c_{j+1}^\dagger c_{j+1} + J_2 c_j^\dagger c_j c_{j+2}^\dagger c_{j+2} \\ &\quad - (J_1 + J_2) c_j^\dagger c_j - J_2 (c_j^\dagger c_{j+1}^\dagger c_{j+1} c_{j+2} + \text{h.c.}) \\ &\quad + \frac{1}{4} J_1 + \frac{1}{4} J_2 \} \end{aligned} \quad (3-5)$$

where "h.c." means the Hermitian conjugate of the preceding expression. The c 's and c^\dagger 's are Fermi operators since they satisfy,

$$\begin{aligned} \{c_i, c_j^\dagger\} &= \delta_{ij} \\ \{c_i, c_j\} &= 0 = \{c_i^\dagger, c_j^\dagger\} \end{aligned} \quad (3-6)$$

It is easy to show that the a 's and a^\dagger 's satisfy Fermi

anticommutation relations at like sites and Bose commutation relations at different sites. By means of the transformation (3-4) we have expressed our Hamiltonian, equation (3-5), in terms of a set of pure Fermi operators, the c 's, whereas before in equation (3-3) it was given in terms of the a 's, a set of Paulions. Also, since $a_j^\dagger a_j = c_j^\dagger c_j$, from (3-4), therefore the expectation value of the number operator $c_j^\dagger c_j$ is the occupation number of the excited state at the j 'th site.

Define the real scalar quantity ϕ_k by,

$$\phi_k \equiv \frac{2\pi k}{N} ; k = 1, 2, \dots, N \quad (3-7)$$

Next we make a Fourier decomposition,

$$c_j = N^{-\frac{1}{2}} \sum_{k=1}^N \exp\{i\phi_k j\} \eta_k \quad (3-8)$$

$$c_j^\dagger = N^{-\frac{1}{2}} \sum_{k=1}^N \exp\{-i\phi_k j\} \eta_k^\dagger$$

The η 's and η^\dagger 's are a new set of Fermi operators since,

$$\{\eta_k, \eta_{k'}^\dagger\} = \delta_{k,k'} \quad (3-9)$$

$$\{\eta_k, \eta_{k'}\} = 0 = \{\eta_k^\dagger, \eta_{k'}^\dagger\}$$

It is easy to show that,

$$\sum_{j=1}^N \exp\{i(\phi_k - \phi_{k'})j\} = N\delta_{\phi_k, \phi_{k'}} = N\delta_{k, k'} \quad ; \quad k, k' = 1, 2, \dots, N \quad (3-10)$$

By generalizing the orthogonality relation (3-10),

$$\sum_{j=1}^N \exp\{i\phi_k j\} = N\bar{\Delta}(\phi_k) \quad (3-11)$$

where,

$$\bar{\Delta}(\phi_k) = \begin{cases} 1, & \text{if } \phi_k = 2\pi n; \quad n=0, \pm 1, \dots \\ 0, & \text{otherwise} \end{cases} \quad (3-12)$$

$\bar{\Delta}(\phi_k)$ is a real scalar function which is even in ϕ_k . Our Hamiltonian (3-5) can now be written as,

$$\begin{aligned} H = & \sum_{k=1}^N \{J_1(\cos\phi_k - 1) + J_2(\cos 2\phi_k - 1)\} \eta_k^\dagger \eta_k \\ & + \frac{N}{4}(J_1 + J_2) + \frac{1}{N} \sum_{\substack{k_1, k_2, k_3, \\ k_4=1}}^N \{J_1 \cos(\phi_{k_1} - \phi_{k_4}) \\ & + J_2 \cos 2(\phi_{k_1} - \phi_{k_4}) - 2J_2 \cos(\phi_{k_1} + \phi_{k_4})\} \\ & \times \bar{\Delta}(\phi_{k_1} + \phi_{k_2} - \phi_{k_3} - \phi_{k_4}) \eta_{k_1}^\dagger \eta_{k_2}^\dagger \eta_{k_3} \eta_{k_4} \end{aligned} \quad (3-13)$$

The physical meaning of introducing the η 's in equations (3-8) is that, by so doing, we have created a set of N

spin waves whose linear momentum is given by ϕ_k in equation (3-7), "k" itself being the wave vector. Since, if $N \rightarrow \infty$, the momentum varies from zero to some finite maximum value, therefore the corresponding wavelengths of the spin waves will go from some finite minimum value to infinity. Ordinary spin waves obey Bose statistics but the spin waves used here differ in that they follow Fermi statistics, equation (3-9).

We introduce a trial Hamiltonian, H_0 , given by,

$$H_0 = \sum_{k=1}^N \epsilon(k) \eta_k^\dagger \eta_k \quad (3-14)$$

where $\epsilon(k)$ is the one-particle energy. The trial Helmholtz free energy, F_t , is defined by,

$$F_t = \langle H \rangle_0 - TS_0 \quad (3-15)$$

where $\langle H \rangle_0$ is the canonical expectation value of H ,

$$\langle H \rangle_0 = \frac{\text{Tr}(e^{-\beta H_0} H)}{\text{Tr}(e^{-\beta H_0})} \quad (3-16)$$

with,

$$\beta = \frac{1}{kT} \quad (3-17)$$

where k is Boltzmann's constant and T is the absolute temperature. S_0 is the entropy of the system described by the trial Hamiltonian (3-14). If the exact Helmholtz

free energy is F , then Bogoliubov's inequality²⁸ states that the trial free energy, F_t , is an upper bound to the exact free energy, F , i.e.

$$F_t \geq F \quad (3-18)$$

We can minimize this upper bound by varying the one-particle energies, $\epsilon(k)$.

The expectation value of the number operator $\eta_k^\dagger \eta_k$ is given by,

$$n_k \equiv \langle \eta_k^\dagger \eta_k \rangle_0 = \frac{1}{1 + e^{\beta \epsilon(k)}} \quad (3-19a)$$

From (3-8) it is easy to show by using (3-10) that,

$$\sum_{j=1}^N c_j^\dagger c_j = \sum_{k=1}^N \eta_k^\dagger \eta_k \quad (3-19b)$$

The η 's, unlike the a 's and the c 's, are not associated with individual sites. We interpret n_k as the occupation number of the spin wave having wave vector " k ". By (3-19a),

$$n_{k,\ell} \equiv \langle \eta_k^\dagger \eta_k \eta_\ell^\dagger \eta_\ell \rangle_0 = (n_\ell + \delta_{k,\ell} n_k e^{\beta \epsilon(k)}) n_k \quad (3-20)$$

Making use of (3-19a) and (3-20) we arrive at the result,

$$\langle \eta_{k_1}^\dagger \eta_{k_2}^\dagger \eta_{k_3} \eta_{k_4} \rangle_0 = \frac{\text{Tr}(e^{-\beta H_0} \eta_{k_1}^\dagger \eta_{k_2}^\dagger \eta_{k_3} \eta_{k_4})}{\text{Tr}(e^{-\beta H_0})}$$

$$= n_{k_1} n_{k_2} (\delta_{k_1, k_4} \delta_{k_2, k_3} - \delta_{k_1, k_3} \delta_{k_2, k_4}) \quad (3-21)$$

We now employ (3-21) to evaluate $\langle H \rangle_0$ defined by equation (3-16). We obtain,

$$\begin{aligned} \frac{\langle H \rangle_0}{N} &= \frac{1}{N} \sum_{k=1}^N \epsilon_0(k) n_k + (J_1 + J_2) \left(\frac{1}{N} \sum_{k=1}^N n_k \right)^2 \\ &- (J_1 - 2J_2) \left(\frac{1}{N} \sum_{k=1}^N n_k \cos \phi_k \right)^2 - J_2 \left(\frac{1}{N} \sum_{k=1}^N n_k \cos 2\phi_k \right)^2 \\ &- 2J_2 \left(\frac{1}{N} \sum_{k=1}^N n_k \right) \left(\frac{1}{N} \sum_{k=1}^N n_k \cos 2\phi_k \right) \\ &- (J_1 + 2J_2) \left(\frac{1}{N} \sum_{k=1}^N n_k \sin \phi_k \right)^2 \\ &- J_2 \left(\frac{1}{N} \sum_{k=1}^N n_k \sin 2\phi_k \right)^2 + \frac{1}{4} J_1 + \frac{1}{4} J_2 \quad (3-22) \end{aligned}$$

where,

$$\epsilon_0(k) = J_1 (\cos \phi_k - 1) + J_2 (\cos 2\phi_k - 1) \quad (3-23)$$

With N an even integer we assume that,

$$\epsilon\left(\frac{N}{2} - k'\right) = \epsilon\left(\frac{N}{2} + k'\right) \quad (3-24a)$$

or,

$$\epsilon(\phi_{k=\pi-\phi_{k'}}) = \epsilon(\phi_{k=\pi+\phi_{k'}}) \quad (3-24b)$$

Thus, we have assumed that the one-particle energies, $\epsilon(k)$, are symmetric with respect to the point $\phi_k = \pi$. A little later we will show that this assumption is consistent with our results.

The assumptions (3-24) imply that,

$$\sum_{k=1}^N n_k \sin \phi_k = 0 = \sum_{k=1}^N n_k \sin 2\phi_k \quad (3-25)$$

Equation (3-22) then reduces to,

$$\begin{aligned} \frac{\langle H \rangle_0}{N} &= \frac{1}{N} \sum_{k=1}^N \epsilon_0(k) n_k + (J_1 + J_2) \left(\frac{1}{N} \sum_{k=1}^N n_k \right)^2 \\ &\quad - (J_1 - 2J_2) \left(\frac{1}{N} \sum_{k=1}^N n_k \cos \phi_k \right)^2 - J_2 \left(\frac{1}{N} \sum_{k=1}^N n_k \cos 2\phi_k \right)^2 \\ &\quad - 2J_2 \left(\frac{1}{N} \sum_{k=1}^N n_k \right) \left(\frac{1}{N} \sum_{k=1}^N n_k \cos 2\phi_k \right) \\ &\quad + \frac{1}{4} J_1 + \frac{1}{4} J_2 \\ &\equiv E'_t \end{aligned} \quad (3-26)$$

where E'_t is the trial energy per site. Now, the entropy per site of the system of noninteracting fermions described by (3-14), S'_0 , is given by,

$$S'_0 = \frac{S_0}{N} = \frac{k}{N} (\ln Q_N + \beta \bar{E}) \quad (3-27)$$

where Q_N is the canonical partition function for the system described by (3-14),

$$Q_N = \text{Tr}(e^{-\beta H_0}) \quad (3-28)$$

and \bar{E} is the expectation value for the energy of the same system,

$$\bar{E} = - \frac{\partial}{\partial \beta} (\ln Q_N) = \langle H_0 \rangle_0 \quad (3-29)$$

Combining these results we find,

$$S_0' = - \frac{k}{N} \sum_{k=1}^N \{ (1-n_k) \ln(1-n_k) + n_k \ln n_k \} \quad (3-30)$$

We rewrite (3-15) as,

$$F_t' = E_t' - TS_0' \quad (3-31)$$

where F_t' is the trial free energy per site. By Bogoliubov's inequality, F_t' is an upper bound to F' , the exact free energy per site, i.e.

$$F_t' \geq F' \quad (3-32)$$

Combining (3-26) and (3-30) in (3-31) we find for the extremum condition $\frac{\partial F_t'}{\partial n_k} = 0$ the equation,

$$\varepsilon(k) = - \frac{2J_2}{\pi} (2S+Q) \cos^2 \phi_k + \left[J_1 - \frac{(J_1 - 2J_2)R}{\pi} \right] \cos \phi_k$$

$$+ \frac{2(J_1 + 2J_2)S}{\pi} \quad (3-33)$$

where,

$$S = \pi \left(\frac{1}{N} \sum_{\ell=1}^N n_{\ell} - \frac{1}{2} \right) \quad (3-34a)$$

$$R = \frac{2\pi}{N} \left(\sum_{\ell=1}^N n_{\ell} \cos \phi_{\ell} \right) \quad (3-34b)$$

$$Q = \frac{2\pi}{N} \left(\sum_{\ell=1}^N n_{\ell} \cos 2\phi_{\ell} \right) \quad (3-34c)$$

We see that S is π times the magnetic moment per spin in the z direction. In the limit as $N \rightarrow \infty$, the summations in equations (3-34) become integrations. From (3-33) it is readily seen that our result is consistent with the assumption $\varepsilon(\phi_k = \pi - \phi_{k'}) = \varepsilon(\phi_k = \pi + \phi_{k'})$. Equation (3-33) is the fundamental non-linear integral equation for $\varepsilon(k)$ in this approximation.

3. Solution For $T = 0$

For $T = 0$ we have the simplification,

$$n_k = \begin{cases} 0, & \text{if } \varepsilon(k) > 0 \\ 1, & \text{if } \varepsilon(k) < 0 \end{cases} \quad (3-35)$$

This allows us to obtain the exact results. (3-32) reduces to,

$$E'_t \geq E'_0 \quad (3-36)$$

The trial energy per site, E'_t , thus becomes an upper bound for the exact ground state energy per site, E'_0 .

We are interested in the case $N \rightarrow \infty$, for which the summations in formulas (3-34) become integrations. As $N \rightarrow \infty$, $\phi_k \rightarrow \phi$ where ϕ is a continuous variable in the closed interval $\{0, 2\pi\}$. When we integrate, we integrate over a certain interval of ϕ , call it I . We choose I to be $\{x, y\}$ and I lies in $\{0, \pi\}$. Since we assumed $\varepsilon(k)$ symmetric with respect to the point $\phi_k = \pi$, equations (3-24), therefore I must also be symmetric with respect to $\phi_k = \pi$ (see Figure 7). Equations (3-34) thus become,

$$S = \int_I d\phi - \frac{\pi}{2} = (y-x) - \frac{\pi}{2} \quad (3-37a)$$

$$R = 2 \int_I \cos \phi d\phi = 2(\sin y - \sin x) \quad (3-37b)$$

$$Q = 2 \int_I \cos 2\phi d\phi = \sin 2y - \sin 2x \quad (3-37c)$$

We must determine the interval I such that when equations (3-37) are substituted into (3-33) one has that $\varepsilon(k) < 0$ when $\phi_k \in I$ and $\varepsilon(k) > 0$ when $\phi_k \notin I$.

There are four cases to consider: (1) $J_1 < 0, J_2 \leq 0$; (2) $J_1 < 0, J_2 > 0$; (3) $J_1 > 0, J_2 \leq 0$; (4) $J_1 > 0, J_2 > 0$. We now define,

$$\alpha \equiv \frac{J_2}{J_1} \quad (3-38)$$

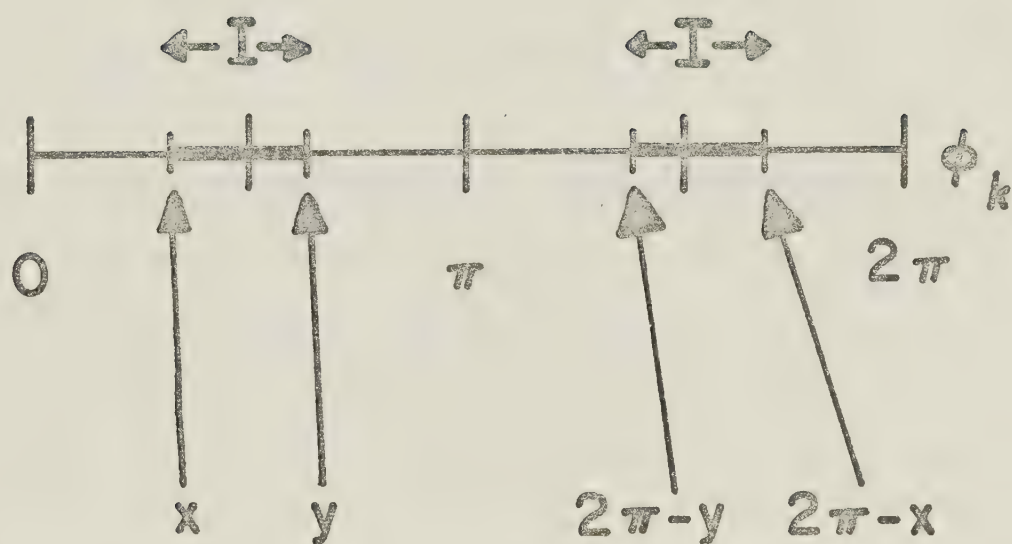
Our definition of α differs slightly from that used by Niemeijer. We shall take $J_1 = +1$ when $J_1 > 0$, and $J_1 = -1$ when $J_1 < 0$. This is clearly not a limitation since α is unrestricted in value, namely $-\infty < \alpha < +\infty$. We can then write (3-33) as,

$$\begin{aligned} \varepsilon(k) = & - \frac{2\alpha J_1}{\pi} (2S+Q) \cos^2 \phi_k + J_1 \left(1 - \frac{(1-2\alpha)R}{\pi} \right) \cos \phi_k \\ & + \frac{2J_1(1+2\alpha)S}{\pi} \end{aligned} \quad (3-39)$$

Equation (3-39) is what we now solve, for different values of $J_1 (= \pm 1)$, and for the whole range of $\alpha (-\infty < \alpha < +\infty)$.

Figure 7: The interval $I = \{x, y\}$, symmetric
about the point $\phi_k = \pi$.

FIGURE 7



A. Ferromagnetic NN Interactions

Nearest neighbour interactions are ferromagnetic for $J_1 < 0$ so we take $J_1 = -1$ and therefore $\alpha = -J_2$. We want the solution of (3-39) for $J_1 = -1$, $-\infty < \alpha < +\infty$. If $I = 0$, namely $x = y$, is the solution then $\varepsilon(k)$ must be positive everywhere and from (3-37), $S = -\pi/2$, $R = Q = 0$. Equation (3-39) becomes,

$$\varepsilon(k) = -2\alpha \cos^2 \phi_k - \cos \phi_k + (1+2\alpha) \quad (3-40a)$$

which factorizes as,

$$\varepsilon(k) = -2\alpha (\cos \phi_k - 1) (\cos \phi_k + 1 + \frac{1}{2\alpha}) \quad (3-40b)$$

Equations (3-40) are plotted for different ranges of α in Figure 8. For $\alpha \geq -\frac{1}{4}$, $\varepsilon(k) > 0$. For $\alpha < -\frac{1}{4}$, however, $\varepsilon(k) < 0$ over part of the range of ϕ_k which means $I = 0$ is no longer the appropriate solution interval. Thus, $I = 0$, namely $x = y$, is the solution of (3-39) for $\alpha \geq -\frac{1}{4}$ when $J_1 = -1$.

The first factor in (3-40b) has two real zeros at $\phi_k = 0, 2\pi$. $I = 0$ is not the solution of (3-39) for $\alpha < -\frac{1}{4}$ because then the second factor in (3-40b) contributes two additional real zeros to $\varepsilon(k)$ in the interval $\{0, 2\pi\}$.

(1) $J_1 = -1$, $0 \leq \alpha < +\infty$ ($J_1 < 0$, $J_2 \leq 0$): $I = 0$ is the solution. Thus, $S = -\pi/2$, $R = Q = 0$. As indicated before, S is π

times the magnetic moment per spin in the z direction.

In the completely ordered state, the magnetic moment per spin in the z direction is $-\frac{1}{2}$, since we have taken the ferromagnetic ground state to be all spins down. Since $S = -\pi/2$, this means that this state is totally ordered. This state, then, is actually the true ground state.

(3-36) thus becomes an equality,

$$E'_t = E'_0 \quad (3-41)$$

The single-particle energy is given by equation (3-40a).

The exact ground state energy per site thus is,

$$E'_t = E'_0 = -\frac{1}{4}(1+\alpha) \quad (3-42)$$

(2) $J_1 = -1$, $-\infty < \alpha < 0$ ($J_1 < 0$, $J_2 > 0$): For $-\frac{1}{4} \leq \alpha < 0$ the solution is still given by $I = 0$; the single-particle energy and trial energy per site are given by (3-40a) and (3-42), respectively. E'_t in equation (3-42), however, is now an upper bound for the exact ground state energy per site rather than the exact energy itself.

For $\alpha < -\frac{1}{4}$ part of the elementary excitation spectrum becomes negative and I is now the interval $\{x, y\}$, as shown in Figure 9. We have restricted ourselves to the interval $\{0, \pi\}$ since $\varepsilon(k)$ is symmetric with respect to the point $\phi_k = \pi$. If we let,

$$\phi_{k_x} = \frac{2\pi k_x}{N} = x \quad (3-43a)$$

$$\phi_{k_Y} = \frac{2\pi k_Y}{N} = y \quad (3-43b)$$

then x and y are to be determined from the equations,

$$\varepsilon(k_x) = 0 \quad (3-44a)$$

$$\varepsilon(k_y) = 0 \quad (3-44b)$$

or, from setting $J_1 = -1$ and using equations (3-37) and (3-39),

$$F_1(x,y)\cos^2 x + F_2(x,y)\cos x + F_3(x,y) = 0 \quad (3-45a)$$

$$F_1(x,y)\cos^2 y + F_2(x,y)\cos y + F_3(x,y) = 0 \quad (3-45b)$$

where,

$$\begin{aligned} F_1(x,y) &= -\alpha(2S + Q) \\ &= -\alpha\{2(y-x) - \pi + (\sin 2y - \sin 2x)\} \end{aligned} \quad (3-46a)$$

$$\begin{aligned} F_2(x,y) &= \pi/2 - \frac{1}{2}(1-2\alpha)R \\ &= \frac{1}{2}\{\pi - 2(1-2\alpha)(\sin y - \sin x)\} \end{aligned} \quad (3-46b)$$

$$\begin{aligned} F_3(x,y) &= (1+2\alpha)S \\ &= \frac{1}{2}(1+2\alpha)\{2(y-x) - \pi\} \end{aligned} \quad (3-46c)$$

Eliminating the physically unacceptable solution $x = y$, i.e. $I = 0$, from the system of equations (3-45) we obtain,

$$F_1(x,y)\cos^2x + F_2(x,y)\cos x + F_3(x,y) = 0 \quad (3-47a)$$

$$F_1(x,y)\{\cos y + \cos x\} + F_2(x,y) = 0 \quad (3-47b)$$

Define the following:

$$a \equiv \frac{y+x}{2} \quad (3-48a)$$

$$b \equiv \frac{y-x}{2} \quad (3-48b)$$

Thus,

$$y = a+b \quad (3-49a)$$

$$x = a-b \quad (3-49b)$$

Since x and y are restricted to the ranges $0 \leq x, y \leq \pi$, then from (3-48) we have $0 \leq a \leq \pi$ and $-\pi/2 \leq b \leq \pi/2$. In terms of the symmetrized variables a and b , system (3-47) becomes,

$$n_1(b)\cos^3a + n_2(b)\cos a - \pi/2 = 0 \quad (3-50a)$$

$$\alpha\{m_3(a,b) - 4b\}m_2(a,b) + m_1(a,b) = 0 \quad (3-50b)$$

where,

$$n_1(b) = 16\alpha \sin b \cos^2 b \quad (3-51a)$$

$$\begin{aligned} n_2(b) = 2(1-2\alpha)\sin b - 2\alpha(\pi-4b)\cos b \\ - 8\alpha \sin b \cos^2 b \end{aligned} \quad (3-51b)$$

and,

$$m_1(a,b) = \frac{1}{2} \cos(a-b) \{ \pi - (1-2\alpha) 4 \cos a \sin b \} \\ - \frac{1}{2} (1+2\alpha) (\pi - 4b) \quad (3-52a)$$

$$m_2(a,b) = \cos^2(a-b) \quad (3-52b)$$

$$m_3(a,b) = \pi - 2 \cos 2a \sin 2b \quad (3-52c)$$

The system of coupled transcendental equations (3-50) has been solved numerically for various values of α in the range $-\infty < \alpha < -\frac{1}{4}$. We have looked for solutions a and b in the ranges $0 \leq a \leq \pi$ and $-\pi/2 \leq b \leq \pi/2$, that is for solutions x and y in the ranges $0 \leq x, y \leq \pi$. Knowing x and y we then calculate the upper bound for the exact ground state energy per site, E'_t in equation (3-26):

$$E'_t = - \{ U - T + T^2 - U^2 + \frac{1}{4} + \alpha (V - T + T^2 + 2U^2 - V^2 - 2TV \\ + \frac{1}{4}) \} \geq E'_0 \quad (3-53)$$

where,

$$T = (y-x)/\pi \quad (3-54a)$$

$$U = (\sin y - \sin x)/\pi \quad (3-54b)$$

$$V = (\sin 2y - \sin 2x)/2\pi \quad (3-54c)$$

Figure 8: $\epsilon(k)$, equations (3-40), as function of ϕ_k for $I = 0$, i.e. $x = y$, for different ranges of α with $J_1 < 0$.

FIGURE 8

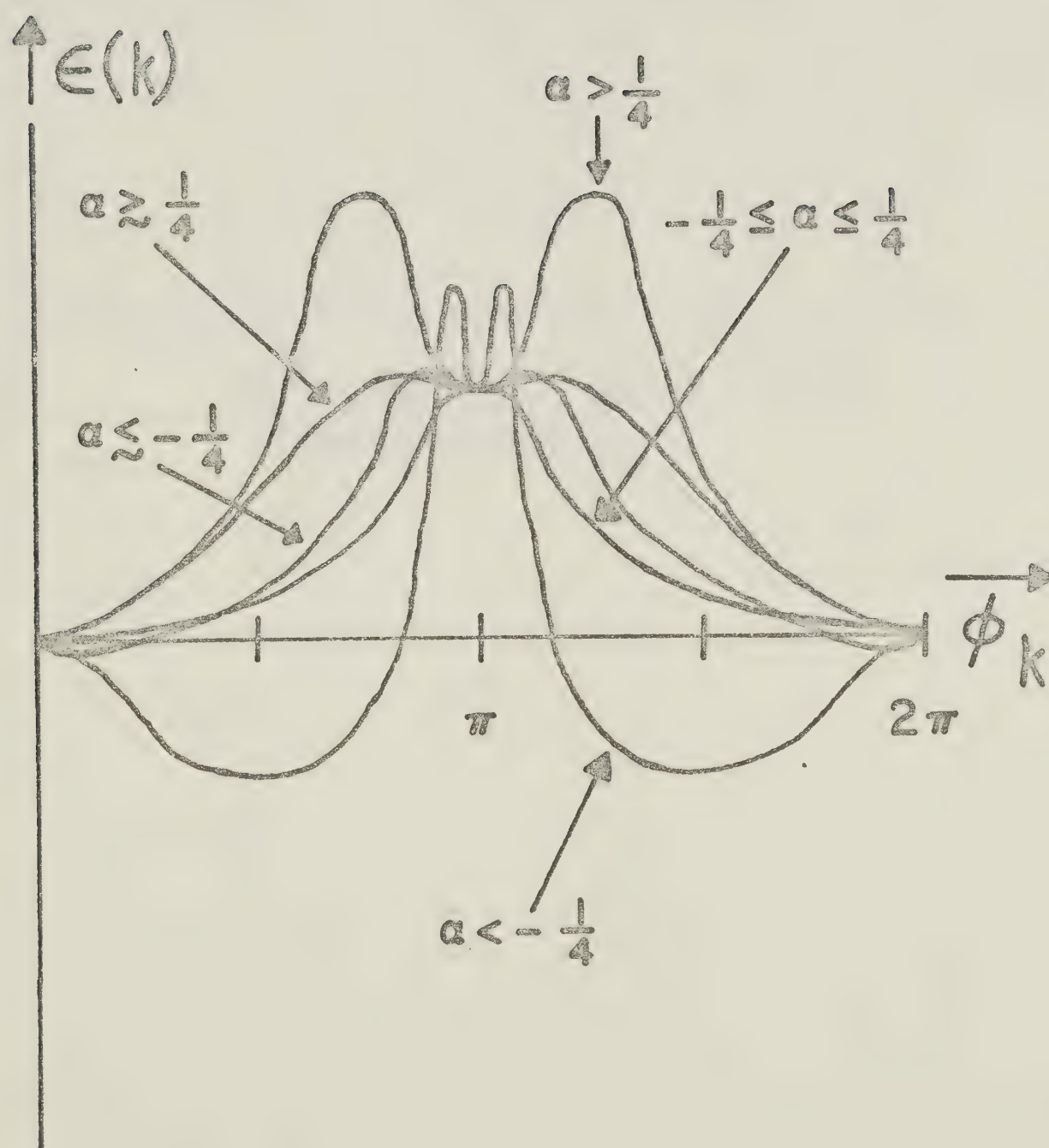
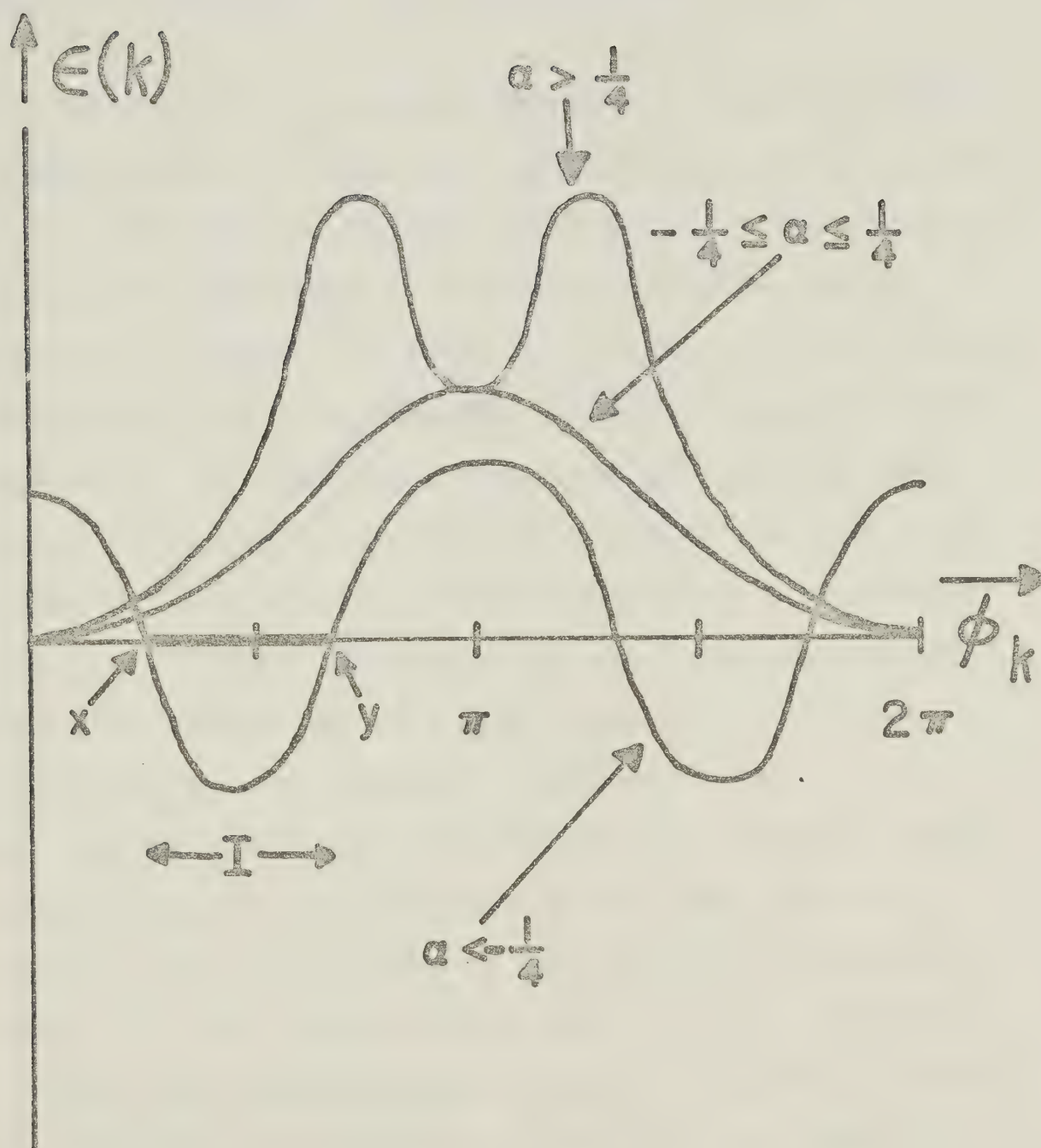


Figure 9: Elementary excitation spectrum, $\epsilon(k)$,
as a function of ϕ_k for different
ranges of α with $J_1 < 0$.

FIGURE 9



For each value of α there are at least two solutions for x and y in the interval $\{0, \pi\}$. The spurious solutions are eliminated by making use of the result that, since the one-particle energies, $\epsilon(k)$, must be symmetric about $\phi_k = \pi$, the interval I must also be symmetric about $\phi_k = \pi$. The results of our calculations, which are identical with those of Niemeijer¹⁰, are given in Table 1.

In Figure 10 the trial energy per site, E'_t , which is an upper bound for the exact ground state energy per site, E'_0 , is plotted as a function of α for $J_1 = -1$. Also included for comparison is the upper bound derived by Majumdar and Ghosh²⁷, namely $E'_t = -\frac{1}{4}(1+\alpha)$; their definitions of J_2 and α are slightly different from the ones used here. For $\alpha \geq 0$ both approximations give the exact ground state energy per site, for $-\frac{1}{4} \leq \alpha < 0$ the same upper bound, but for $\alpha < -\frac{1}{4}$ our upper bound gives a much better result. The first derivative of the trial energy per site with respect to α is continuous at $\alpha = -\frac{1}{4}$; the second derivative, however, is discontinuous: We see that the nature of the upper bound for the exact ground state energy per site changes at the same value of α , namely $\alpha = -\frac{1}{4}$, as it does in the classical Heisenberg chain. In this approximation then, $\alpha = -\frac{1}{4}$ is the point at which the antiferromagnetic second neighbour interactions become strong enough to alter the ferromagnetic ground state.

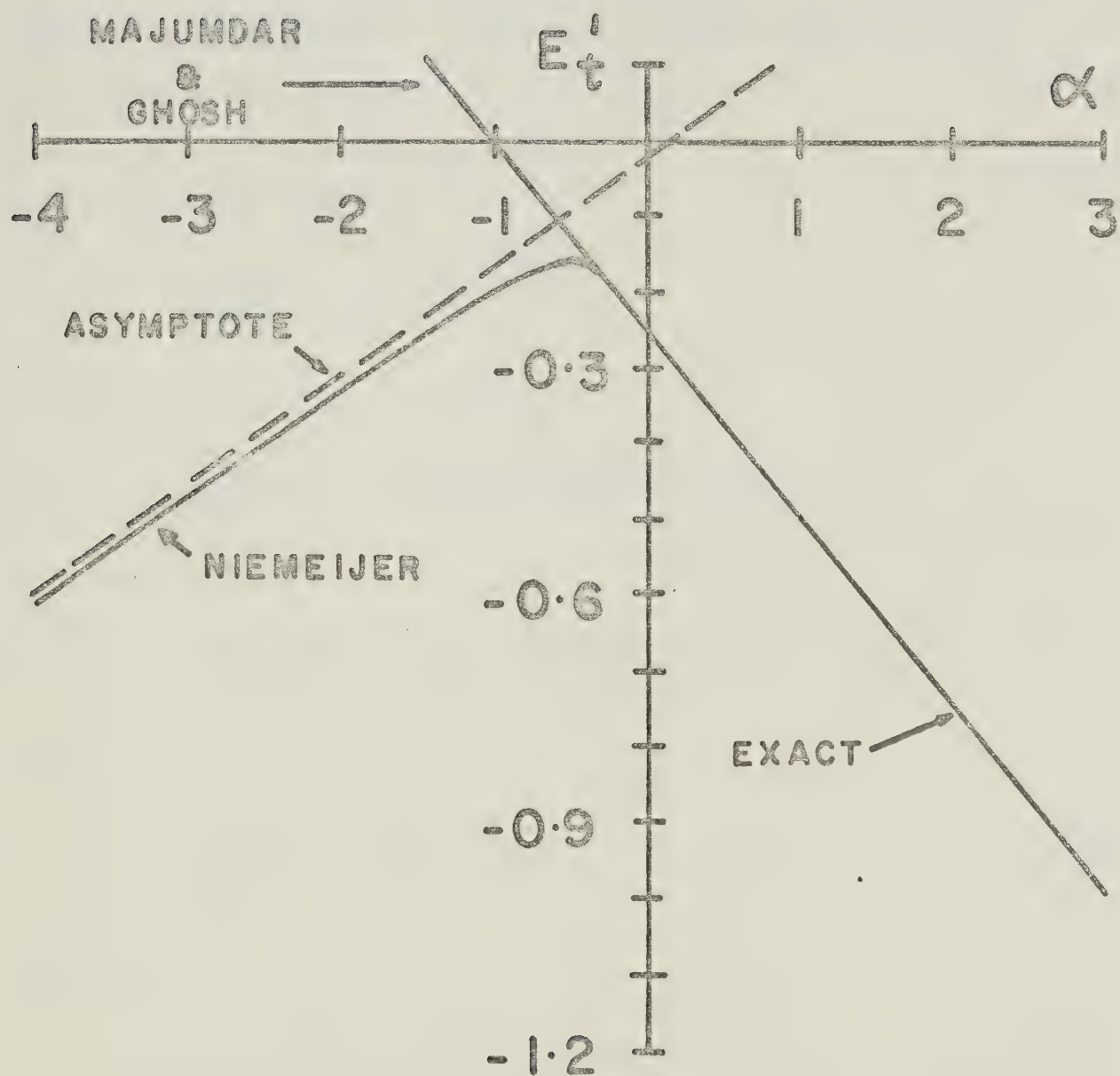
Table 1: Numerical solutions of equations
(3 - 50) for various values of α
with corresponding E'_t

Table 1

α	x (radians)	y (radians)	E'_t
-0.26	0.215914	0.255793	-0.185005
-0.30	0.469102	0.654895	-0.175500
-0.35	0.632849	1.02837	-0.166171
-0.40	0.695777	1.30736	-0.161076
-0.45	0.719143	1.47114	-0.159422
-0.50	0.736543	1.57080	-0.159818
-0.55	0.752498	1.63896	-0.161506
-0.60	0.767143	1.68966	-0.164093
-0.65	0.780414	1.72948	-0.167351
-0.70	0.792365	1.76194	-0.171129
-0.75	0.803112	1.78912	-0.175323
-0.80	0.812790	1.81232	-0.179857
-0.85	0.821530	1.83246	-0.184675
-0.90	0.829449	1.85013	-0.189731
-0.95	0.836652	1.86580	-0.194991
-1.0	0.843227	1.87982	-0.200426
-1.5	0.886869	1.96790	-0.260779
-2	0.910043	2.01241	-0.326636
-3	0.934246	2.05799	-0.464345
-5	0.954467	2.09564	-0.747501
-10	0.970220	2.12482	-1.46508
-100	0.984898	2.15196	-14.4573
-1000	0.986394	2.15472	-144.421

Figure 10: Upper bounds for the exact ground state energy per site for an infinite chain with $J_1 < 0$, as a function of α . For Niemeijer's result, asymptote for large negative α is plotted.

FIGURE 10



We now want to find the asymptote to the E'_t versus α curve for $J_1 < 0$ (Figure 10) for large negative α . First we define,

$$\beta \equiv \frac{1}{\alpha} \quad (3-55)$$

Using the fact that $x = x(\beta)$, $y = y(\beta)$, and dividing (3-47) by α we obtain,

$$f(x(\beta), y(\beta), \beta) = 0 \quad (3-56a)$$

$$g(x(\beta), y(\beta), \beta) = 0 \quad (3-56b)$$

where,

$$\begin{aligned} f(x, y, \beta) = G_1(x, y) \cos^2 x + G_2(x, y) \cos x \\ + G_3(x, y) \end{aligned} \quad (3-57a)$$

$$g(x, y, \beta) = G_1(x, y) \{ \cos x + \cos y \} + G_2(x, y) \quad (3-57b)$$

and,

$$G_i(x, y) = \beta F_i(x, y) ; i = 1, 2, 3 \quad (3-58)$$

Define,

$$E = E(x(\beta), y(\beta), \beta) \equiv \beta E'_t \quad (3-59)$$

where E'_t is given in equation (3-53). When $\alpha \rightarrow -\infty$, i.e. $\beta \rightarrow 0^-$, x and y (also a and b) approach certain values, say x_∞ and y_∞ (a_∞ and b_∞). Multiplying through equations

(3-50) by β and letting $\beta \rightarrow 0^-$ we have,

$$\begin{aligned} & (\pi - 2\cos 2a_\infty \sin 2b_\infty - 4b_\infty) \cos^2(a_\infty - b_\infty) \\ & + 4\cos(a_\infty - b_\infty) \cos a_\infty \sin b_\infty - (\pi - 4b_\infty) = 0 \quad (3-60a) \end{aligned}$$

$$\begin{aligned} & 16\sin b_\infty \cos^2 b_\infty \cos^3 a_\infty - \{4\sin b_\infty + 2(\pi - 4b_\infty) \cos b_\infty \\ & + 8\sin b_\infty \cos^2 b_\infty\} \cos a_\infty = 0 \quad (3-60b) \end{aligned}$$

From these we obtain,

$$\cos a_\infty = 0 \quad (3-61a)$$

$$4\sin^3 b_\infty - (\pi - 4b_\infty) \cos b_\infty = 0 \quad (3-61b)$$

whose solutions in the allowed ranges of a and b are $a_\infty = \pi/2$ radians, $b_\infty = 0.584236$ radians. Then from (3-49), $x_\infty = 0.986530$ radians and $y_\infty = 2.15506$ radians.

We expand $x(\beta)$, $y(\beta)$ and $E(x(\beta), y(\beta), \beta)$ in a Taylor series about $\beta = 0^-$ as follows:

$$x(\beta) = x_\infty + A_1 \beta + O(\beta^2) + \dots \quad (3-62a)$$

$$y(\beta) = y_\infty + B_1 \beta + O(\beta^2) + \dots \quad (3-62b)$$

$$E(x(\beta), y(\beta), \beta) = C_0 + C_1 \beta + O(\beta^2) + \dots \quad (3-62c)$$

Not knowing x and y explicitly as functions of β , we cannot find the coefficients A_1 and B_1 by direct differentiation; instead, we use equations (3-56). Substituting

the first two of equations (3-62) into (3-56), we expand the left hand sides of the two equations in a Taylor series in β about $\beta = 0^-$. Then, equating coefficients of equal powers of β on both sides, we find to first order,

$$\left(\frac{\partial f}{\partial x} A_1 + \frac{\partial f}{\partial y} B_1 + \frac{\partial f}{\partial \beta} \right)_{\beta=0^-} = 0 \quad (3-63a)$$

$$\left(\frac{\partial g}{\partial x} A_1 + \frac{\partial g}{\partial y} B_1 + \frac{\partial g}{\partial \beta} \right)_{\beta=0^-} = 0 \quad (3-63b)$$

Solving this system of two linear equations in the two unknowns A_1 and B_1 we have,

$$A_1 = \frac{\left(\frac{\partial f}{\partial y} \right)_{\beta=0^-} \left(\frac{\partial g}{\partial \beta} \right)_{\beta=0^-} - \left(\frac{\partial f}{\partial \beta} \right)_{\beta=0^-} \left(\frac{\partial g}{\partial y} \right)_{\beta=0^-}}{\left(\frac{\partial f}{\partial x} \right)_{\beta=0^-} \left(\frac{\partial g}{\partial y} \right)_{\beta=0^-} - \left(\frac{\partial f}{\partial y} \right)_{\beta=0^-} \left(\frac{\partial g}{\partial x} \right)_{\beta=0^-}} \quad (3-64a)$$

$$B_1 = \frac{\left(\frac{\partial f}{\partial \beta} \right)_{\beta=0^-} \left(\frac{\partial g}{\partial x} \right)_{\beta=0^-} - \left(\frac{\partial f}{\partial x} \right)_{\beta=0^-} \left(\frac{\partial g}{\partial \beta} \right)_{\beta=0^-}}{\left(\frac{\partial f}{\partial x} \right)_{\beta=0^-} \left(\frac{\partial g}{\partial y} \right)_{\beta=0^-} - \left(\frac{\partial f}{\partial y} \right)_{\beta=0^-} \left(\frac{\partial g}{\partial x} \right)_{\beta=0^-}} \quad (3-64b)$$

If we also substitute the first two of equations (3-62) into the third and expand the left hand side in a Taylor series in β about $\beta = 0^-$ and compare with the right hand side, then to first order,

$$C_0 = E(x_\infty, y_\infty, 0^-) \quad (3-65)$$

and,

$$C_1 = A_1 \left[\frac{\partial E}{\partial x} \right]_{\beta=0^-} + B_1 \left[\frac{\partial E}{\partial y} \right]_{\beta=0^-} + \left[\frac{\partial E}{\partial \beta} \right]_{\beta=0^-} \quad (3-66)$$

We can rewrite (3-62c) in the form,

$$E'_t = \alpha C_0 + C_1 + O(1/\alpha) + \dots \quad (3-67)$$

From (3-67) we see that the equation of the asymptote for large negative α is,

$$E'_t = \alpha C_0 + C_1 \quad (3-68)$$

so C_0 is the slope and C_1 is the E'_t intercept of the asymptote. Performing the numerical calculations we get,

$$x(\beta) = 0.986530 + 0.111949\beta + O(\beta^2) + \dots \quad (3-69a)$$

$$y(\beta) = 2.15506 + 0.362710\beta + O(\beta^2) + \dots \quad (3-69b)$$

$$E(x(\beta), y(\beta), \beta) = 0.144405 - 0.0164042\beta + O(\beta^2) + \dots \quad (3-69c)$$

and the equation of the asymptote is,

$$E'_t = 0.144405\alpha - 0.0164042 \quad (3-70)$$

The asymptote is shown in Figure 10.

B. Antiferromagnetic NN Interactions

For $J_1 > 0$, nearest neighbour interactions are anti-ferromagnetic so we take $J_1 = +1$ and therefore $\alpha = +J_2$. We want the solution of (3-39) for $J_1 = +1$, $-\infty < \alpha < +\infty$. Niemeijer¹⁰ has said that $I = \{\pi/2, \pi\}$ is the solution for all values of α . This, however, is not correct.

If $I = \{\pi/2, \pi\}$ is the solution then from (3-37) we have $S = Q = 0$, $R = -2$. Equation (3-39) becomes,

$$\varepsilon(k) = \left(1 + \frac{2}{\pi}(1-2\alpha)\right) \cos\phi_k \quad (3-71)$$

For $\alpha < \frac{1}{2} + \pi/4$ (≈ 1.28540) the coefficient of " $\cos\phi_k$ " in (3-71) is positive, for $\alpha > \frac{1}{2} + \pi/4$ it is negative and for $\alpha = \frac{1}{2} + \pi/4$ it is zero.

Thus, $I = \{\pi/2, \pi\}$ is a solution of (3-39) for $\alpha < \frac{1}{2} + \pi/4$ when $J_1 = +1$ but, for $\alpha \geq \frac{1}{2} + \pi/4$, $I = \{\pi/2, \pi\}$ cannot be a solution since, if it is, then $\varepsilon(k) > 0$ when $\phi_k \in I$ and $\varepsilon(k) < 0$ when $\phi_k \notin I$, which is contrary to what we assumed about the properties of the solution interval I . For $\alpha \geq \frac{1}{2} + \pi/4$ we look for a different solution interval.

Niemeijer's results have that the upper bound for the exact ground state energy per site approaches $+\infty$ as $\alpha \rightarrow +\infty$. Since the upper bound approached $-\infty$ as $\alpha \rightarrow \pm\infty$ for the ferromagnetic nn case, Stephenson²⁹ suggested that E_t' should exhibit a similar behaviour for the antiferromagnetic nn case. This speculation led to the discovery of the error in Niemeijer's results.

(3) $J_1 = +1$, $-\infty < \alpha \leq 0$ ($J_1 > 0$, $J_2 \leq 0$): $I = \{\pi/2, \pi\}$ is the solution. Thus, $S = Q = 0$, $R = -2$. The elementary excitation spectrum (single-particle energy) is given by equation (3-71). The upper bound for the exact ground state energy per site is, from (3-26),

$$E'_t = -\frac{1}{\pi} \left(1 + \frac{1}{\pi} (1-2\alpha) \right) \geq E'_0 \quad (3-72)$$

So far we agree with Niemeijer's calculations.

(4) $J_1 = +1$, $0 < \alpha < +\infty$ ($J_1 > 0$, $J_2 > 0$): For $0 < \alpha < \frac{1}{2} + \pi/4$ a possible solution is still given by $I = \{\pi/2, \pi\}$ in which case equations (3-71) and (3-72) give the elementary excitation spectrum and trial energy per site, respectively.

For $\alpha \geq \frac{1}{2} + \pi/4$ the interval I is now $\{x, y\}$, as shown in Figure 11. Again we restrict ourselves to the interval $\{0, \pi\}$ since $\epsilon(k)$ is still symmetric about $\phi_k = \pi$. Following the same procedure as in Case (2) we obtain, after eliminating the solution $x = y$,

$$F_1(x, y) \cos^2 x + F_2(x, y) \cos x + F_3(x, y) = 0 \quad (3-73a)$$

$$F_1(x, y) \{\cos y + \cos x\} + F_2(x, y) = 0 \quad (3-73b)$$

where F_1 , F_2 , F_3 are defined as before. System (3-73) is identical with system (3-47). If we solve (3-73) numerically for x and y we can then find the trial energy per site from (3-26):

$$E'_t = U - T + T^2 - U^2 + \frac{1}{4} + \alpha (V - T + T^2 + 2U^2 - V^2 - 2TV + \frac{1}{4}) \geq E'_0 \quad (3-74)$$

where T, U, V are defined by (3-54).

System (3-73) has no solutions in the allowed ranges of x and y , $0 \leq x, y \leq \pi$, for $-\frac{1}{4} \leq \alpha \leq 1$ but does have valid solutions for all $\alpha \geq 1$. We have already shown that $I = \{\pi/2, \pi\}$ is a possible solution of equation (3-39) for $0 < \alpha < \frac{1}{2} + \pi/4$. The actual solutions of (3-39) for Case (4) thus are:

- a). $I = \{\pi/2, \pi\}$, for $0 < \alpha \leq 1$.
- b). $I = \{x, y\}$, where x and y are determined by the system of equations (3-47), for $\alpha \geq \frac{1}{2} + \pi/4$.
- c). Either $I = \{\pi/2, \pi\}$ or $I = \{x, y\}$, whichever has the lower trial energy per site, for $1 \leq \alpha < \frac{1}{2} + \pi/4$.

E'_t from (3-72) and E'_t from (3-74) intersect when $\alpha \approx 1.05$. For $1 \leq \alpha \leq 1.05$ equation (3-72) gives the lower trial energy per site while for $1.05 \leq \alpha < \frac{1}{2} + \pi/4$ it is (3-74). Thus, $I = \{\pi/2, \pi\}$ is the solution interval for $1 \leq \alpha \leq 1.05$ and for $1.05 \leq \alpha < \frac{1}{2} + \pi/4$ it is $I = \{x, y\}$.

Numerical solutions of system (3-73) for various values of α in the range $1.05 \leq \alpha < +\infty$ are given in Table 2.

Figure 11: Elementary excitation spectrum, $\varepsilon(k)$,
as function of ϕ_k for different ranges
of α with $J_1 > 0$.

FIGURE II

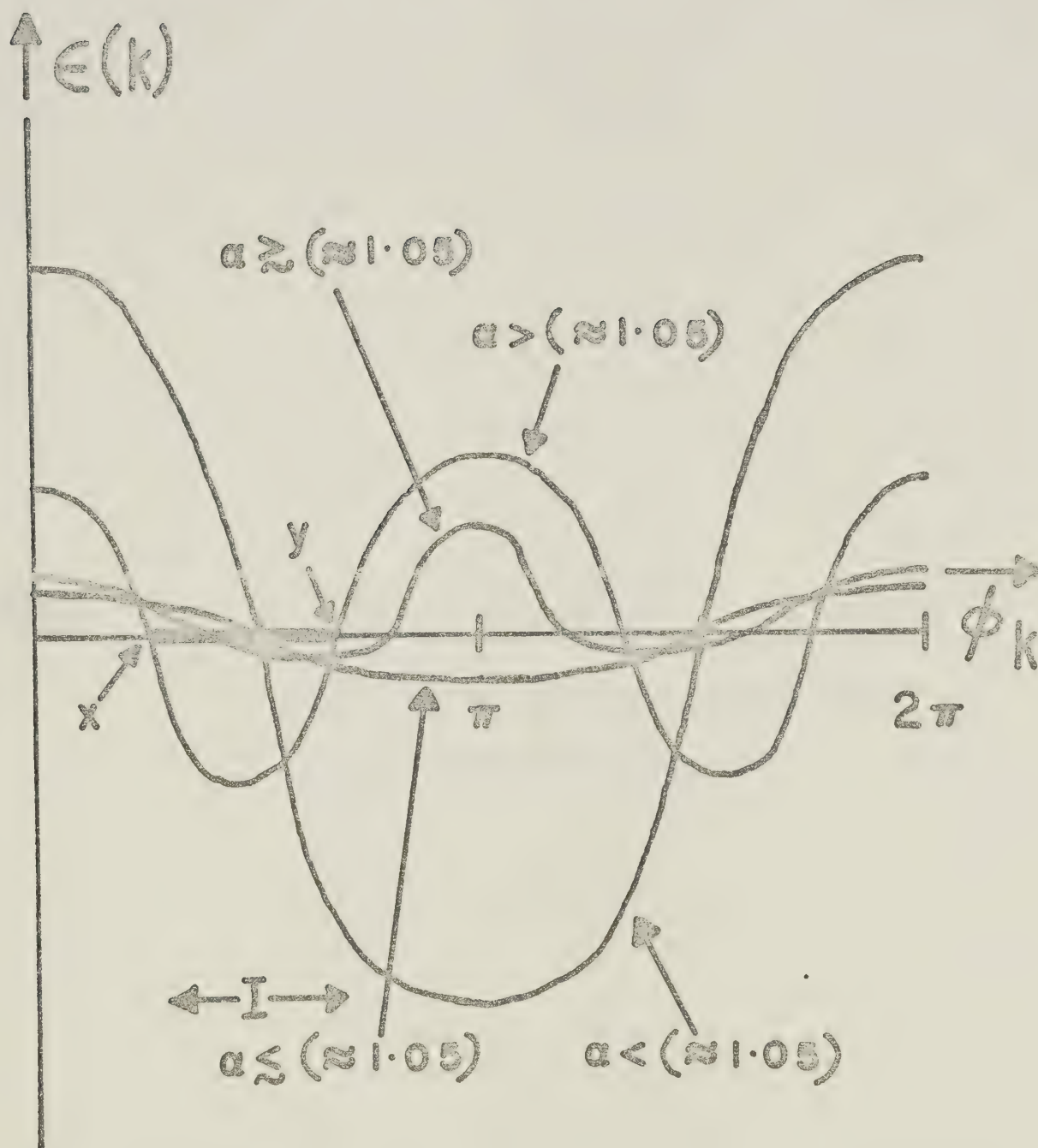


Table 2: Numerical solutions of equations
(3 - 73) for various values of α
with corresponding E'_t

Table 2

α	x (radians)	y (radians)	E'_t
1.1	1.21591	2.58948	-0.202938
1.2	1.17933	2.51871	-0.209671
$\frac{1}{2} + \frac{\pi}{4}$	1.15851	2.47852	-0.217019
1.3	1.15550	2.47272	-0.218379
1.4	1.13786	2.43884	-0.228308
1.5	1.12401	2.41233	-0.239077
1.6	1.11271	2.39080	-0.250458
1.7	1.10327	2.37387	-0.262302
1.8	1.09523	2.35764	-0.274510
1.9	1.08828	2.34451	-0.287007
2	1.08221	2.33306	-0.299738
2.5	1.06043	2.29217	-0.365757
3	1.04686	2.26682	-0.434077
4	1.03074	2.23682	-0.573857
5	1.02144	2.21957	-0.715597
7.5	1.00944	2.19734	-1.07317
10	1.00359	2.18651	-1.43251
100	0.988231	2.18512	-14.4245
1000	0.986727	2.15534	-144.388

In Figure 12 we have plotted the trial energy per site, E'_t , as a function of α , $J_1 = +1$, for the results of Majumdar and Ghosh²⁷, Niemeijer¹⁰ and ourselves (equation (3-72) and Table 2). For $\alpha \lesssim 1.05$ we have rederived Niemeijer's upper bound; however, for $\alpha \gtrsim 1.05$ our upper bound is considerably better. The upper bound for the exact ground state energy per site that we obtained as a correction to the work of Niemeijer is continuous at the point of intersection, $\alpha \approx 1.05$, but its first derivative with respect to α exhibits a discontinuity there. Niemeijer's and our upper bounds are both much better than that given by Majumdar and Ghosh. For $\alpha = 0$, (3-72) gives $E'_t(\alpha=0) \approx -0.419631 \geq E'_0$ and this agrees with the result of Bulaevskii³⁰. The well known exact result due to Hulthén²² is $E'_0(\alpha=0) = -\ln 2 + \frac{1}{4} \approx -0.44315$.

Finally we want to find the asymptote to our E'_t versus α curve for $J_1 > 0$ (Figure 12) for large positive α . We proceed as we did in finding the asymptote for the case $J_1 < 0$. Comparing (3-53) and (3-74),

$$(E'_t)_{J_1 > 0} = - (E'_t)_{J_1 < 0} \quad (3-75)$$

When $\alpha \rightarrow +\infty$, i.e. $\beta \rightarrow 0^+$, x and y approach x_∞ and y_∞ , respectively, where $x_\infty = 0.986530$ radians and $y_\infty = 2.15506$ radians, as before. We make Taylor expansions of $x(\beta)$, $y(\beta)$ and $E(x(\beta), y(\beta), \beta)$. Proceeding as for $J_1 < 0$

and comparing we observe that,

$$\left(\frac{\partial E}{\partial x_i} \right)_{\substack{\beta=0^+ \\ J_1 > 0}} = - \left(\frac{\partial E}{\partial x_i} \right)_{\substack{\beta=0^- \\ J_1 < 0}} ; i = 1, 2, 3 \quad (3-76)$$

where $x_1 = x$, $x_2 = y$, $x_3 = \beta$, and,

$$\{E(x_\infty, y_\infty, 0^+)\}_{J_1 > 0} = - \{E(x_\infty, y_\infty, 0^-)\}_{J_1 < 0} \quad (3-77)$$

We find,

$$(A_1)_{J_1 > 0} = (A_1)_{J_1 < 0} \quad (3-78a)$$

$$(B_1)_{J_1 > 0} = (B_1)_{J_1 < 0} \quad (3-78b)$$

and,

$$(C_i)_{J_1 > 0} = - (C_i)_{J_1 < 0} ; i = 0, 1 \quad (3-79)$$

The Taylor expansions for $x(\beta)$ and $y(\beta)$ are identical with (3-69a) and (3-69b), respectively. However, for $E(x(\beta), y(\beta), \beta)$ we have,

$$\begin{aligned} E(x(\beta), y(\beta), \beta) &= -0.144405 + 0.0164042\beta \\ &\quad + O(\beta^2) + \dots \end{aligned} \quad (3-80)$$

The equation of the asymptote is found to be,

$$E'_t = -0.144405\alpha + 0.0164042 \quad (3-81)$$

This is just the negative of the asymptote we had for $J_1 < 0$, equation (3-70). The asymptote (3-81) is shown in Figure 12.

Note Added In Proof: For the ferromagnetic nn case $I = 0$ is the solution for $\alpha \geq -\frac{1}{4}$. By inspection we see that $I = 0$ is a valid solution interval for large ferromagnetic second neighbour interactions when first neighbour interactions are small, and of either sign. For large ferromagnetic J_2 , nnn spins will be aligned. In the present approximation, nn spins are aligned also, even when $J_1 > 0$. For large ferromagnetic J_2 the excitation spectrum is,

$$\epsilon(k) = 2\alpha(\cos\phi_k - 1)\left(\cos\phi_k + 1 + \frac{1}{2\alpha}\right) \quad (3-82)$$

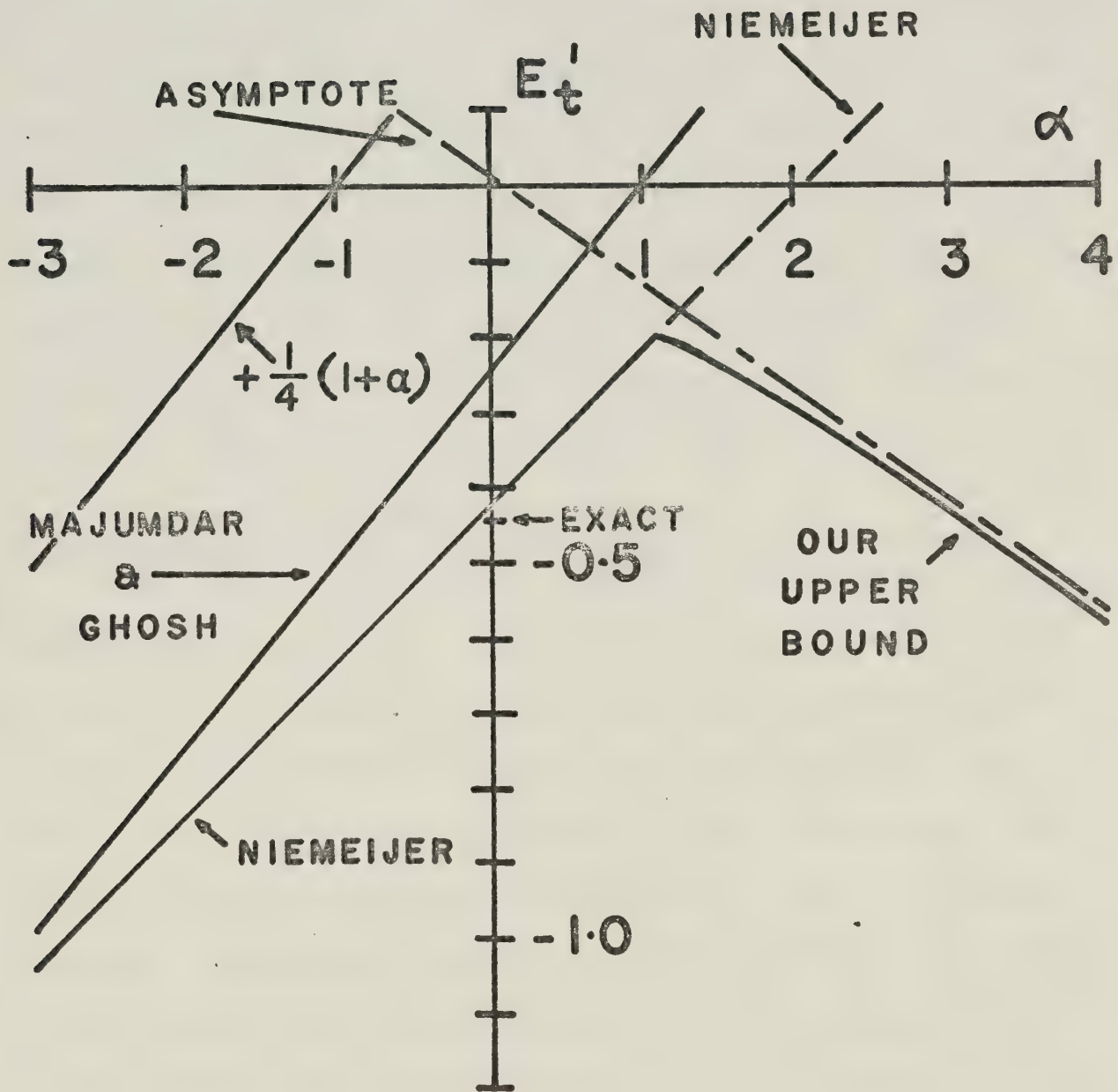
and the trial energy per site is,

$$E'_t = +\frac{1}{4}(1+\alpha) \geq E'_0 \quad (3-83)$$

Equations (3-72) and (3-83) for E'_t intersect when $\alpha \approx -14.14$. E'_t in (3-83) has the correct asymptotic slope as $\alpha \rightarrow -\infty$ and is included in Figure 12.

Figure 12: Upper bounds for the exact ground state energy per site for an infinite chain with $J_1 > 0$, as a function of α . For our result, asymptote for large positive α is plotted.

FIGURE 12



Chapter IV. Conclusion

In this thesis we have introduced and studied certain properties of two one-dimensional lattice models. For the spin $\frac{1}{2}$ one-dimensional Ising model having both nn and nnn interactions in zero magnetic field, the canonical partition function has been found using the transfer matrix method and an equation for its locus of zeros was then obtained as a function of λ , the ratio of the next nearest to the nearest neighbour interaction energy. The equation was solved numerically for different λ values and the results were plotted in Figures 1-6. We then discussed general properties of the loci of zeros and investigated exactly soluble cases.

Also considered was the one-dimensional spin $\frac{1}{2}$ zero field Heisenberg model. Reviewing the work of Niemeijer, by means of a temperature dependent Hartree-Fock approximation we were able to derive an upper bound for the exact ground state energy per site at zero temperature for various different values of the nearest and next nearest neighbour interaction energies. After showing that part of the upper bound given by Niemeijer for the antiferromagnetic nearest neighbour case ($J_1 > 0$) was wrong, we were able to obtain the correct upper bound, which was considerably better than that of Niemeijer. With $\alpha = J_2/J_1$, we also found the asymptote to the upper bound as a function of α for large negative α with $J_1 < 0$ and for large positive

α with $J_1 > 0$.

As indicated by Niemeijer this variational method that was applied to the zero field Heisenberg model can be quite readily extended to the problem where there is a non-zero magnetic field present in the z (Cartesian coordinate z) axis.

In this thesis we have introduced next nearest neighbour interactions into two one-dimensional lattice models in an attempt to bring them perhaps a little bit closer to describing an actual physical system. The solutions we have obtained will, it is hoped, shed more light on ideas about lattice systems and on as yet unsolved lattice models.

Bibliography

1. E. Ising, Z. Physik 31, 253(1925)
2. L. Onsager, Phys. Rev. 65, 117(1944)
3. E. Lieb, T. Schultz and D. Mattis, An. Phys. 16, 407(1961)
4. S. Katsura, Phys. Rev. 127, 1508(1962)
5. T. H. Berlin and M. Kac, Phys. Rev. 86, 821(1952)
6. R. I. Joseph, Phys. Rev. 138, A1441(1965)
7. G. A. T. Allen and D. D. Betts, Proc. Phys. Soc. 91, 341(1967)
8. I. Dzyaloshinsky, J. Phys. Chem. Solids 4, 241(1958)
9. S. Wong, S. T. Dembiński and W. Opechowski, Physica 42, 565(1969)
10. Th. Niemeijer, J. Math. Phys. 12, 1487(1971)
11. M. Suzuki, Prog. Theor. Phys. 38, 1225(1967)
12. C. N. Yang and T. D. Lee, Phys. Rev. 87, 404(1952)
13. J. Stephenson, Can. J. Phys. 48, 1724(1970)
14. G. L. Jones, J. Math. Phys. 7, 2000(1966)
15. E. W. Montroll, J. Chem. Phys. 10, 61(1942)
16. T. Obokata and T. Oguchi, J. Phys. Soc. Japan 25, 322(1968)
17. T. Oguchi, J. Phys. Soc. Japan 20, 2236(1965)
18. S. Katsura and M. Ohminami, J. Phys. A 5, 95(1972)
19. J. F. Dobson, J. Math. Phys. 10, 40(1969)
20. C. Domb, Advan. Phys. 9, Nos. 34,35, p.149(1960)
21. H. A. Bethe, Z. Physik 71, 205(1931)
22. L. Hulthén, Arkiv. Mat. Astron. Fysik 26A, 1(1938)
23. R. Orbach, Phys. Rev. 112, 309(1958)

24. T. A. Kaplan, Phys. Rev. 116, 888(1955)
25. K. Yoshida and H. Miwa, J. Appl. Phys. 32, Suppl. No. 3, 8S(1961)
26. I. Ono, Phys. Letts. 38A, 327(1972)
27. C. K. Majumdar and D. K. Ghosh, J. Math. Phys. 10, 1932(1969)
28. N. N. Bogoliubov, unpublished work, see Footnote 4 of Z. V. Tolmachev, Dokl. Akad. Nauk. SSSR 134, 1324(1960) (Sov. Phys. Dokl. 5, 984(1961))
29. J. Stephenson, private communication
30. L. N. Bulaevskii, Zh. Exp. Teor. Fiz. 43, 968(1962) (Sov. Phys. JETP 16, 685(1963))
31. J. Stephenson, unpublished work

Appendix

In this appendix we discuss boundary conditions and the locus of zeros of the partition function (2-4) in Chapter 2 in order to remove any ambiguities that may exist. Equation (2-4) gives the canonical partition function of an N spin $\frac{1}{2}$ one-dimensional Ising linear chain having both nearest and next nearest neighbour interactions present in zero magnetic field. We rewrite this as,

$$Z_N^{\text{lc}}(K_1, K_2, 0) = \sum_{\sigma_1=-1}^1 \dots \sum_{\sigma_N=-1}^1 \exp(K_1 \sum_{i=1}^{N-1} \sigma_i \sigma_{i+1} + K_2 \sum_{i=1}^{N-2} \sigma_i \sigma_{i+2}) \quad (\text{A-1})$$

where the superscript "lc" indicates that linear chain boundary conditions are used. Dobson's result, (2-5), becomes,

$$Z_N^{\text{lc}}(K_1, K_2, 0) = 2 Z_{N-1}^{\text{lc}}(K_2, 0, K_1) \quad (\text{A-2})$$

To evaluate the $N-1$ spin partition function, $Z_{N-1}(K_2, 0, K_1)$, we used the transfer matrix approach; however, it is well known that to use a transfer matrix in the manner that we did in equation (2-11), one must assume cyclic boundary conditions, i.e. the linear chain has now become a ring. We then set this $N-1$ spin function equal to zero to obtain its locus of zeros so we actually found the

zeros of,

$$z_{N-1}^{\text{ring}}(K_2, 0, K_1) = 0 \quad (\text{A-3})$$

where the superscript "ring" means that cyclic boundary conditions were employed.

We now derive a relation between the partition function of a linear chain and that of a ring. We have,

$$z_{N-1}^{\ell c}(K_2, 0, K_1) = \sum_{\text{all states}} \exp(-\beta H_{N-1}^{\ell c}) \quad (\text{A-4a})$$

$$z_{N-1}^{\text{ring}}(K_2, 0, K_1) = \sum_{\text{all states}} \exp(-\beta H_{N-1}^{\text{ring}}) \quad (\text{A-4b})$$

where,

$$-\beta H_{N-1}^{\ell c} = K_2 \sum_{i=1}^{N-2} \sigma_i \sigma_{i+1} + K_1 \sum_{i=1}^{N-1} \sigma_i \quad (\text{A-5a})$$

$$-\beta H_{N-1}^{\text{ring}} = K_2 \sum_{i=1}^{N-1} \sigma_i \sigma_{i+1} + K_1 \sum_{i=1}^{N-1} \sigma_i \quad (\text{A-5b})$$

We notice that,

$$z_{N-1}^{\ell c}(K_2, 0, K_1) = \sum_{\text{all states}} \exp(-\beta H_{N-1}^{\text{ring}}) \exp(-K_2 \sigma_{N-1} \sigma_N) \quad (\text{A-6})$$

Since $\exp(-K_2 \sigma_{N-1} \sigma_N) = \cosh K_2 - \sigma_{N-1} \sigma_N \sinh K_2$, this becomes,

$$\begin{aligned}
z_{N-1}^{\text{lc}}(K_2, 0, K_1) &= z_{N-1}^{\text{ring}}(K_2, 0, K_1) \{ \cosh K_2 \\
&\quad - \sinh K_2 \langle \sigma_{N-1} \sigma_N \rangle_{N-1}^{\text{ring}}(K_2, 0, K_1) \}
\end{aligned}
\tag{A-7}$$

where $\langle \sigma_{N-1} \sigma_N \rangle_{N-1}^{\text{ring}}(K_2, 0, K_1)$ is the two-spin correlation function between spins at sites $N-1$ and N (i.e. site 1) on a ring of $N-1$ spins. Because of translational symmetry on the ring,

$$\langle \sigma_{N-1} \sigma_N \rangle_{N-1}^{\text{ring}} = \langle \sigma_1 \sigma_2 \rangle_{N-1}^{\text{ring}} = \langle \sigma_2 \sigma_3 \rangle_{N-1}^{\text{ring}} = \dots \tag{A-8}$$

Defining,

$$\omega_1(K_2, 0, K_1) \equiv \langle \sigma_1 \sigma_2 \rangle_{N-1}^{\text{ring}}(K_2, 0, K_1) \tag{A-9}$$

(A-7) can be written as,

$$\begin{aligned}
z_{N-1}^{\text{lc}}(K_2, 0, K_1) &= z_{N-1}^{\text{ring}}(K_2, 0, K_1) \{ \cosh K_2 \\
&\quad - \sinh K_2 \omega_1(K_2, 0, K_1) \}
\end{aligned}
\tag{A-10}$$

Now,

$$z_{N-1}^{\text{ring}}(K_2, 0, K_1) = \lambda_+^{N-1} + \lambda_-^{N-1} \tag{A-11}$$

where λ_{\pm} are defined in equation (2-15). It can be shown³¹ that,

$$z_{N-1}^{\text{ring}}(K_2, 0, K_1) \omega_1(K_2, 0, K_1) = \lambda_+^{N-1} (x^2 + y^2 \gamma) + \lambda_-^{N-1} (x^2 + y^2 / \gamma) \quad (\text{A-12})$$

where,

$$x = \text{magnetization} = \frac{1 - \mu_1}{\{(1 - \mu_1)^2 + 4\mu_1 z_1^2\}^{1/2}} \quad (\text{A-13a})$$

$$y = \frac{2\mu_1^{1/2} z_1}{\{(1 - \mu_1)^2 + 4\mu_1 z_1^2\}^{1/2}} \quad (\text{A-13b})$$

and,

$$\mu_1 = e^{-2K_1} \quad (\text{A-14a})$$

$$z_1 = e^{-2K_2} \quad (\text{A-14b})$$

$$\gamma = \frac{\lambda_-}{\lambda_+} \quad (\text{A-14c})$$

Equation (A-10) thus becomes,

$$z_{N-1}^{\text{lc}}(K_2, 0, K_1) = \lambda_+^{N-1} \{\cosh K_2 - \sinh K_2 (x^2 + y^2 \gamma)\} + \lambda_-^{N-1} \{\cosh K_2 - \sinh K_2 (x^2 + y^2 / \gamma)\} \quad (\text{A-15})$$

Setting (A-15) to zero we obtain as our locus of zeros,

$$\frac{\lambda_+}{\lambda_-} = (-1)^{1/N-1} D^{1/N-1} \quad (\text{A-16})$$

where,

$$D = \frac{\cosh K_2 - \sinh K_2 (x^2 + y^2 / \gamma)}{\cosh K_2 - \sinh K_2 (x^2 + y^2 \gamma)} \quad (\text{A-17})$$

Recall,

$$(-1)^{1/N-1} = \exp\left(\frac{i(2k+1)\pi}{N-1}\right) ; k=0,1,\dots,N-2 \quad (\text{A-18})$$

We can rewrite (A-16) as,

$$\frac{\lambda_+}{\lambda_-} = (-1)^{1/N-1} |D|^{1/N-1} \exp\left(\frac{i}{N} \arg D\right) \quad (\text{A-19})$$

We are interested in the case $N \rightarrow \infty$. For this, $(-1)^{1/N-1}$ becomes continuous along the unit circle, $|D|^{1/N-1} \rightarrow 1$ and $\exp\left(\frac{i}{N} \arg D\right) \rightarrow 1$. Thus, as $N \rightarrow \infty$,

$$\frac{\lambda_+}{\lambda_-} = (-1)^{1/N-1} \quad (\text{A-20})$$

(A-20) is the locus of zeros, as $N \rightarrow \infty$, obtained from,

$$Z_{N-1}^{\ell C}(K_2, 0, K_1) = 0 \quad (\text{A-21})$$

The equation that we actually solved numerically was,
from (2-17),

$$\frac{\lambda_+}{\lambda_-} = (-1)^{1/N-1}$$

which is the exact locus of zeros for all N obtained from,

$$z_{N-1}^{\text{ring}}(K_2, 0, K_1) = 0 \quad (\text{A-3})$$

Thus we see that our procedure of getting the locus of zeros of the linear chain $(z_N^{\text{lc}}(K_1, K_2, 0) = 2z_{N-1}^{\text{lc}}(K_2, 0, K_1))$ by solving for the zeros of the ring $(z_{N-1}^{\text{ring}}(K_2, 0, K_1))$ was a valid one.

In conclusion we look at two limiting cases of equation (A-10). First consider $\lambda = 0$. Therefore, $K_2 = \lambda K_1 = 0$. We have,

$$\begin{aligned} z_{N-1}^{\text{lc}}(0, 0, K_1) &= (2\cosh K_1)^{N-1} \\ &= z_{N-1}^{\text{ring}}(0, 0, K_1) \end{aligned} \quad (\text{A-22})$$

The locus of zeros of (A-22) in the complex $z = e^{-2K_1}$ plane is the point $z = -1$. Our numerical results bear this out; we found that as $\lambda \rightarrow 0$ our locus of zeros did shrink to the point $z = -1$ (see Figures 1-6).

Finally we look at $K_1 = 0$, namely the zero field case. We have,

$$\begin{aligned} z_{N-1}^{\text{lc}}(K_2, 0, 0) &= 2(2\cosh K_2)^{N-2} \\ &= 2z_{N-1}^{\text{ring}}(K_2, 0, 0) \{ \cosh K_2 \\ &\quad - \sinh K_2 \omega_1(K_2, 0, 0) \} \end{aligned} \quad (\text{A-23})$$

The locus of zeros of (A-23) in the complex $z' = e^{-2K_2}$ plane is the point $z' = -1$. For both the ring and the linear chain we solve (A-20) to obtain the locus:

$$\frac{\lambda_+}{\lambda_-} = (-1)^{1/N-1} \quad (\text{A-20})$$

(A-20) is exact for all N and for only $N \rightarrow \infty$ for the ring and for the chain, respectively. For the ring in zero field we know that we should have the unit circle as our locus in the z' plane (this is obtained by setting $K_1 = 0$ in equation (A-20) and solving). For the linear chain we had only the point $z' = -1$, from (A-23), whereas from (A-20) we should expect to have a unit circle. This apparent contradiction, however, is readily reconcilable. Recall that for the chain the exact result for all N for the locus of zeros was given by equation (A-16). However, $D = 0$ when $K_1 = 0$ so for the chain when $K_1 = 0$ we are actually solving,

$$\frac{\lambda_+}{\lambda_-} = 0 \quad (\text{A-24})$$

which has the solution $z' = -1$, thus reconciling the two different approaches.

B30066